

# Target Reflectivity

*John F. Shaeffer*

## Chapter Outline

6.1	Introduction .....	211
6.2	Basic Reflection Physics .....	212
6.3	Radar Cross Section Definition .....	219
6.4	Three Scattering Regimes .....	224
6.5	High-Frequency Scattering .....	227
6.6	Examples .....	236
6.7	Further Reading .....	244
6.8	References .....	244
6.9	Problems .....	245

## 6.1 | INTRODUCTION

The basic motivation for this chapter is to describe a key link in the understanding of radar: how does a radar wave, more properly known as an electromagnetic (EM) wave, transmitted from some transmitter source, interact with a target to produce reflected energy at some receiver position? The goals for this chapter are as follows:

1. To understand what an electromagnetic wave is.
2. To understand its properties.
3. To describe a measure of the amount of reflected energy, a quantity known as radar cross section (RCS).
4. To understand basic scattering or reflectivity physics.
5. To focus on the typical microwave scattering mechanisms.
6. To understand how two or more scattering centers add and subtract.
7. To illustrate examples of high-frequency scattering from targets along with scattering center images.

## 6.2 | BASIC REFLECTION PHYSICS

Basic reflection physics must start with a description of the characteristics of an electromagnetic wave and then progress to how this EM wave interacts with a target object to cause reflection.

### 6.2.1 Electromagnetic Wave Fundamentals

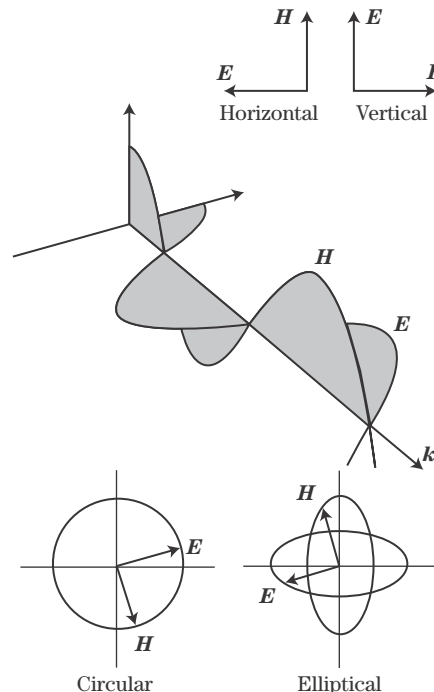
An electromagnetic wave is the self-propagating transport of energy (voltage and current) through space, without this energy being attached or directed via some external structure such as a transmission line or waveguide. James Clerk Maxwell showed in the 1860s that a time-changing electric field,  $E$  (V/m), is the source for the magnetic field,  $H$  (A/m), and, in turn, a time-changing  $H$  is the source for  $E$ . Thus, once an EM wave is launched, it becomes self-propagating. EM waves propagate in free space as well as inside material media.

The three most important characteristics of an EM wave (Figure 6-1) are (1) its frequency or rate of temporal variation,  $f$ , with units of hertz (Hz or cycles/s); (2) its wavelength or spatial variation,  $\lambda$ , with units of meters (m); and (3) its velocity of propagation,  $v$ , with units of meters per second (m/s). These three fundamental wave quantities are not independent; they are related as

$$\lambda f = v \quad (6.1)$$

When an EM wave propagates in free space,  $v = c$ , the velocity of light, which is approximately  $3 \times 10^8$  m/s. Mathematically it is given by the free space values of electric

**FIGURE 6-1** ■ Snapshot of an EM wave in time and allowed polarization directions (from Knott [1]).



permittivity,  $\epsilon_0$ , and magnetic permeability,  $\mu_0$ :

$$c = \frac{1}{\sqrt{\epsilon_0 \mu_0}} \approx 3 \times 10^8 \text{ m/s} \quad (6.2)$$

which is about 1 foot per nanosecond, or about 1,000 feet per microsecond.

EM waves propagating inside a material media travel slower than in free space with a velocity

$$v = \frac{c}{n} = \frac{1}{\sqrt{\epsilon_m \mu_m}} \quad (6.3)$$

where  $n$  is the material index of refraction, a composite measure of electric energy storage, and is a function of the material electric and magnetic energy storage properties characterized by its relative dielectric permittivity,  $\epsilon_m$  (electric energy storage), and permeability,  $\mu_m$  (magnetic energy storage). Thus, the more energy that can be stored inside a material, the slower an EM wave will propagate. Also, inside a material, the time variation of the wave is the same as in free space, but the wavelength becomes smaller to always satisfy the relation  $\lambda f = v$ . In free space a wave is typically characterized by either its frequency or wavelength, whereas inside a material the wave is typically characterized by its frequency.

Frequency and wavelength may also be characterized by radian frequency,  $\omega = 2\pi f$ , and by wave number,  $k = 2\pi/\lambda$ , and the relationship  $\lambda f = v$  becomes  $\omega/k = v$ .

For the sake of analysis a fictional plane wave is often considered, given mathematically by

$$\begin{aligned} \mathbf{E} &= \mathbf{E}_0 e^{j(\omega t - \mathbf{k} \cdot \mathbf{R})} \\ \text{or} \\ \mathbf{H} &= \mathbf{H}_0 e^{j(\omega t - \mathbf{k} \cdot \mathbf{R})} \end{aligned} \quad (6.4)$$

where the spatial phase  $\mathbf{k} \cdot \mathbf{R}$  is the distance from some origin measured in units of wavelength  $\lambda$  in the direction of propagation  $\mathbf{k}$ . The nature of the sinusoidal temporal and spatial variation is shown within the complex phasor exponent  $(\omega t - \mathbf{k} \cdot \mathbf{R})$ . The constant phase fronts of this plane wave are perpendicular to the direction of propagation  $\mathbf{k}$ . Recall from geometry that a plane in space is defined by  $\mathbf{k} \cdot \mathbf{R} = \text{constant}$ , where  $\mathbf{k}$  is normal to the plane, and  $\mathbf{R}$  is a vector to a point on the plane.

The electric and magnetic fields  $\mathbf{E}$  and  $\mathbf{H}$  are time-varying vector quantities. The quantities  $\mathbf{E}_0$  and  $\mathbf{H}_0$  are their vector “amplitudes.” While these are in general three-dimensional vectors, for plane waves the component in the direction of propagation  $\mathbf{k}$  is zero, so  $\mathbf{E}_0$  and  $\mathbf{H}_0$  will be considered to be two-dimensional vector quantities.

This plane wave is fictional because its intensity does not fall off as the wave propagates away from its source and because it has exactly planar wave fronts. A spherical wave at a sufficient distance from its source can be considered planar over the target dimensions. In addition, there is insignificant  $1/R$  decrease in intensity over the relatively small target. Thus, the plane wave concept is a practical simplification for waves interacting with targets.

Three fundamental vectors characterize an EM wave:

- The electric field,  $\mathbf{E}$ , with units of V/m.
- The magnetic field,  $\mathbf{H}$ , with units of A/m.
- The direction of propagation,  $\mathbf{k}$ , the vector wavenumber, whose magnitude (also called the scalar wavenumber or just the wavenumber) is  $2\pi/\lambda$ , with units of rad/m.

Once an EM wave is launched so that  $\mathbf{E}$  and  $\mathbf{H}$  are no longer attached to some sort of conducting structure, the  $\mathbf{E}$  and  $\mathbf{H}$  fields circle and close back on themselves, and the fields are now solenoidal.

In free space, there is equal energy in the wave  $\mathbf{E}$  and  $\mathbf{H}$  field components so that time-changing  $\mathbf{E}$  is the source for  $\mathbf{H}$  and vice versa. While there is equal energy contained in each field component, the numerical values of  $\mathbf{E}$  and  $\mathbf{H}$  are not the same. The ratio of the norm of  $\mathbf{E}$  to the norm of  $\mathbf{H}$  is the wave impedance,  $Z$ , which in free space is the constant value of approximately 377 ohms. This numerical value results from using the SI system of units:

$$\frac{\|\mathbf{E}\|}{\|\mathbf{H}\|} = Z = \sqrt{\frac{\mu_0}{\epsilon_0}} \approx 377 \text{ ohms}$$

Because this ratio is constant, this free space wave can be characterized by either its electric or magnetic field component.

Maxwell's equations for propagating waves require that the spatial directions of  $\mathbf{E}$ ,  $\mathbf{H}$ , and  $\mathbf{k}$  be perpendicular to each other (Figure 6-1) so that  $\mathbf{E}$  and  $\mathbf{H}$  must always be perpendicular to the direction of propagation and be perpendicular to each other. In free space  $\mathbf{E}$  and  $\mathbf{H}$  are in phase; that is, each peaks at the same time. However, inside a material media, where energy storage occurs, this is often not the case.

An EM wave transports electrical energy characterized as an energy flux (i.e., energy per unit cross section area,  $\text{W/m}^2$ ). The magnitude and direction of the energy flux are given by the Poynting vector,  $\mathbf{P}$ , which is the vector cross product of  $\mathbf{E}$  and  $\mathbf{H}$ . Averaged over time,  $\mathbf{P}$  is

$$\mathbf{P} = \frac{1}{2} \text{Real}(\mathbf{E} \times \mathbf{H}^*) \text{ W/m}^2 \quad (6.5)$$

where  $\mathbf{H}^*$  is the complex conjugate of  $\mathbf{H}$ .

### 6.2.2 Electromagnetic Wave Polarization

Another characteristic of an EM wave is its polarization, which is the direction of its electric field vector  $\mathbf{E}$ . Maxwell's equations require only that  $\mathbf{E}$ ,  $\mathbf{H}$ , and  $\mathbf{k}$  be perpendicular. Thus,  $\mathbf{E}$  may point in any direction in a plane perpendicular to the direction of propagation  $\mathbf{k}$  (Figure 6-1). Polarization may be linear where the direction  $\mathbf{E}$  is always in the same direction, or it may be circular (or more generally, elliptical) where  $\mathbf{E}$  and  $\mathbf{H}$  rotate as the wave propagates.

Linear polarization is specified typically as relative to one's surroundings (Figure 6-2). In the real world with the earth as a reference, horizontal or vertical are usually chosen as linear polarization directions. In the computational world with spherical coordinates, polarization is specified in the azimuth,  $\phi$ , and polar,  $\theta$ , directions.

Circular polarization is specified as left or right circular, counterclockwise (LC) or clockwise (RC) rotation of  $\mathbf{E}$ , respectively. The reference for LC or RC is determined by looking in the direction of propagation  $\mathbf{k}$  and sensing which way  $\mathbf{E}$  is rotating. For transmission, the sense is based on looking *away* from the antenna (outgoing wave), and for reception it is based on looking *toward* the antenna (incoming wave) [2].

Polarization information is required to describe how an EM wave is both transmitted and received. The physical characteristics of the transmitting antenna that launches an EM

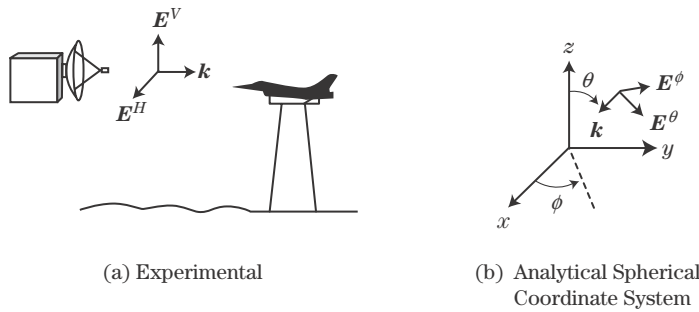


**FIGURE 6-2** ■ Polarization convention is given by the direction of  $E$  relative to local surroundings [1].

wave determine the polarization of the outgoing wave. The receiving antenna polarization characteristic determines the amount of signal actually received from an incoming EM wave of a given polarization. Thus, RCS becomes a function of both transmitter polarization and receiver polarization. In addition, some target reflection properties such as edges and surface waves are a function of the polarization of the incident wave relative to target geometry.

For transmitting, a horizontal dipole radiates an EM wave with horizontal polarization, whereas a vertical dipole launches a wave with vertical polarization. For receiving, a horizontal dipole responds only to the horizontal component of the incoming EM wave polarization, whereas a vertical dipole is sensitive only to the wave's vertical component of polarization.

### 6.2.3 Electromagnetic Wave Reflection

A discussion of EM wave reflection, the familiar “echo” of radar signals, requires consideration of boundary conditions, induced currents, re-radiation, and Maxwell's equations. In optics, high-frequency scattering waves reflect according to Snell's law such that the angle of reflection is equal to the angle of incidence, much the same way a billiard ball bounces. This section discusses the physics of how this behavior arises.

For simplicity, consider a perfect electric conductor (PEC). A PEC has infinite conductivity. Its surface is always at the same electric potential and cannot support a tangential electric field; that is, the PEC surface is a short circuit to any applied electric field because charge is free to move under an applied electric field (force). When a PEC surface is completely closed, there can be no electric field inside the surface; that is, the closed surface becomes a perfect shield called a Faraday shield.

It is customary to split the total vector electric field into the *incident field* and *scattered field*  $E^{inc}$  and  $E^{scat}$ . The total electric field is  $E^{total} = E^{inc} + E^{scat}$ . The incident field comes from some distant source, whereas the scattered field is due to currents and charges on the scattering body. The PEC boundary condition of zero tangential field applies to  $E^{total}$ , that is, to the tangential sum of the incident and scattered fields. It can be expressed mathematically as

$$E^{total} \cdot n = (E^{inc} + E^{scat}) \cdot n = 0 \quad (6.6)$$

where  $n$  is a unit vector normal to the surface. Thus, the tangential scattered field is always equal and opposite in direction and amplitude to the incident tangential incident field at the PEC surface. Electric field lines of the local scattered field begin and end on surface-induced charges. At the surface the  $E^{total}$  field must be perpendicular to the surface.

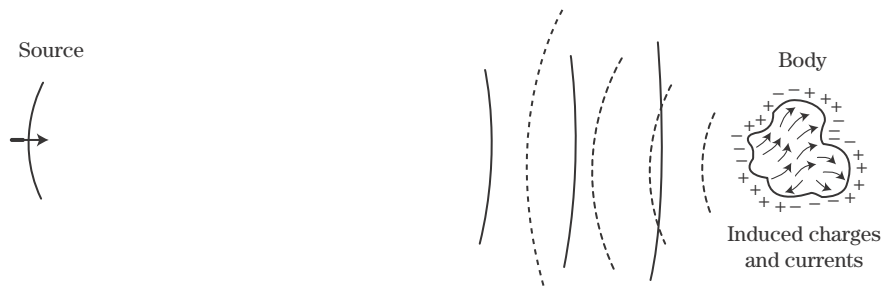


**FIGURE 6-3** ■ Charges and currents: are induced on a PEC to satisfy the perfect conductor boundary conditions of zero tangential field (short circuit); and, consequently, re-radiate a scattered field  $E^{scat}$ . From Knott [3].

With no applied  $E^{inc}$  field, there are no induced electric charges on the PEC, and  $E^{scat}$  is zero. Now, say at time  $t = 0$ , a *static* electric field  $E^{inc}$  is applied. Because the PEC is a short circuit, there is an immediate separation of electric charge on the surface, + and –, which creates a scattered field  $E^{scat}$ . The nature of the induced charge separation is such that the boundary condition of zero tangential field is now satisfied everywhere on the conducting surface in accordance with equation (6.6).

For this static applied field the instant after  $t = 0$ , electric charges have been induced, the boundary conditions have been satisfied, and nothing more happens because the total tangential field is zero:  $\mathbf{n} \cdot E^{scat} = -\mathbf{n} \cdot E^{inc}$ . Now consider what happens if an EM wave is incident on the PEC rather than a static field (Figure 6-3). The PEC is exposed to a time-varying  $E^{inc}$  field as the wave propagates over the surface. Because the surface must be a short circuit, the induced scattered field,  $E^{scat}$ , and the induced electric charge distribution must vary with time so as to always satisfy the boundary conditions of equation (6.6). The creation of the induced electric charge by the incident field and the resulting induced scattered field required to satisfy equation (6.6) is the fundamental physical process by which the zero tangential total electric field boundary condition is satisfied.

As a result of the applied EM wave, the induced charges are constantly in time motion. Because current is nothing more than charge in motion, the EM wave also creates induced currents. These currents and charges, which form fundamentally to create a tangential scattered field on the surface of the PEC that is exactly opposite the incident field, now act like antenna sources in that they radiate the scattered field far beyond the PEC itself.

Maxwell's equations in integral form show how the scattered field is formed from the PEC induced surface currents,  $\mathbf{J}$  (A/m), and charge density,  $\rho_s$  (coulombs/m<sup>2</sup>).

$$E^{scat}(\mathbf{R}_f) = \int \left( -j\omega\mu \mathbf{J} g + \frac{\rho_s}{\epsilon} \nabla g \right) dS \quad (6.7)$$

This form of Maxwell's equations, where time harmonic waves  $\exp(j\omega t)$  have been assumed, shows that the scattered electric field vector  $E^{scat}$  at spatial field position  $\mathbf{R}_f$  is computed as the sum over the surface currents  $\mathbf{J}$  and charges  $\rho$ . When field point  $\mathbf{R}_f$  is on the PEC surface, the surface tangential component of  $E^{scat}$  is exactly equal and opposite of the tangential incident field such that the total surface tangential field is zero as required for a short circuit surface.

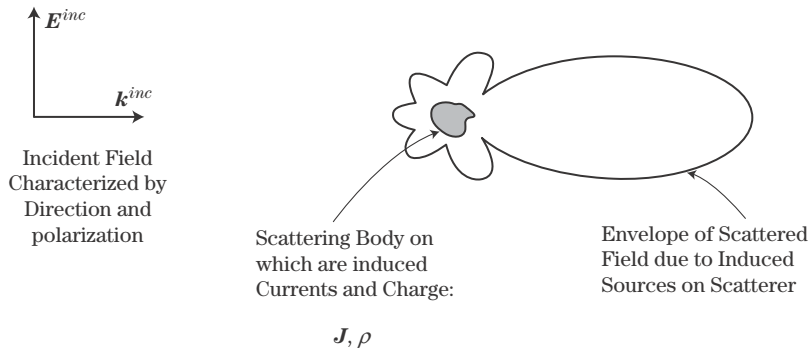


**FIGURE 6-4** ■ PEC induced currents and charges reradiate a scattered field [1].

The  $g$  term in this equation is the Green's function, which relates a source quantity  $J$  or  $\rho$  at a surface source location  $R_s$  to the field  $E$  at spatial point  $R_f$ . The Green's function is

$$g = \frac{e^{-jk \cdot (R_f - R_s)}}{4\pi |R_f - R_s|} \quad (6.8)$$

and can be thought of as a Huygen's wavelet in that it describes how a source at position  $R_s$  influences the field at position  $R_f$ . The denominator is the  $1/R$  falloff of intensity. The numerator is the phase or time delay from the source disturbance to influence the field point. The argument of the complex exponential is proportional to distance from a surface source point to the spatial point where the scattered field is being evaluated. This distance is measured in units of wavelength,  $kR = 2\pi R/\lambda$ .

While the primary function of the induced sources (charges and currents) is to satisfy the boundary conditions, those sources also act as antenna sources in that they radiate fields far away from the surface. This is the scattered wave (Figure 6-4).

A PEC sphere can be used as an example of how an incident wave induces sources on the surface that satisfy the boundary conditions and the resulting scattered and total fields surrounding the sphere. Figure 6-5 shows a time snapshot of currents induced on a sphere illuminated from the right with vertical polarization. The maximum current zone is where the incident wave first hits the sphere, and behind this point the surface creeping wave currents can be seen.

The induced currents and charges reradiate (i.e., become the source) for the scattered fields shown in Figure 6-6. In this figure the view is changed such that the incident wave

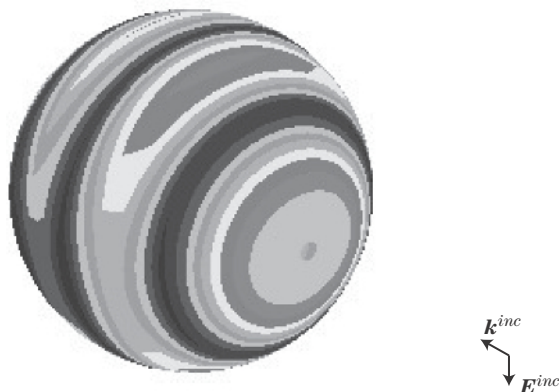
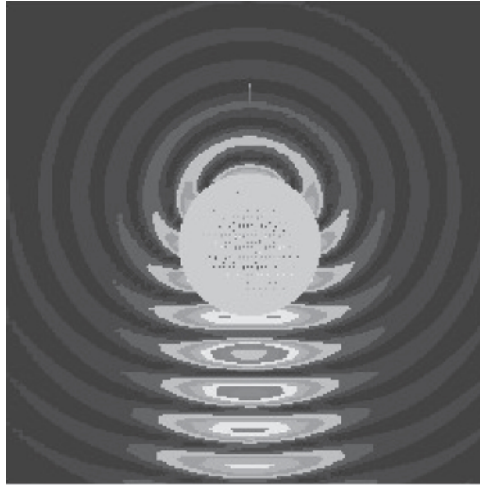


**FIGURE 6-5** ■ Time snapshot of currents induced on a sphere due to an incident plane wave with vertical polarization.



**FIGURE 6-6** ■ Time snapshot of scattered fields from currents on a PEC sphere illuminated from the top.

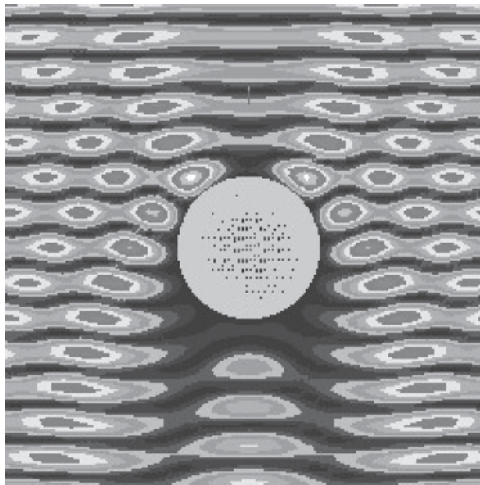


is traveling from top to bottom over the sphere. There are three important things to note: (1) A scattered spherical wave is created traveling out from the sphere; (2) inside the sphere, partially masked by the graphic, is a strong horizontal field; and (3) behind the sphere (bottom of the figure) is a strong forward scattered field. This scattered field is propagating in *all* spatial directions away from the surface. This includes the direction back to the original source of the incoming plane wave (i.e., the backscatter direction).

Figure 6-6 shows the scattered field. Adding back the incident plane wave gives the total field (Figure 6-7). This figure shows the obvious incident plane wave and the important physics of how the scattered field and incident field add to zero inside the conducting surface and, behind the sphere, create a shadow on the side opposite the incident wave.

To illustrate this for a slightly more complicated object, Figure 6-8 shows the currents and scattered field from a PEC cylinder with an ogive nose when illuminated from 20 degrees above and from the left with the polarization in the plane of the figure. Clearly seen is the forward scattered field, which, when added to the incident field, forms a shadow behind. The figure also shows a strong scattered field in the specular direction from the

**FIGURE 6-7** ■ Time snapshot of the total  $E$  field,  $E^{tot} = E^{scat} + E^{inc}$ , when sphere is illuminated from the top with a plane wave  $E^{inc}$ .





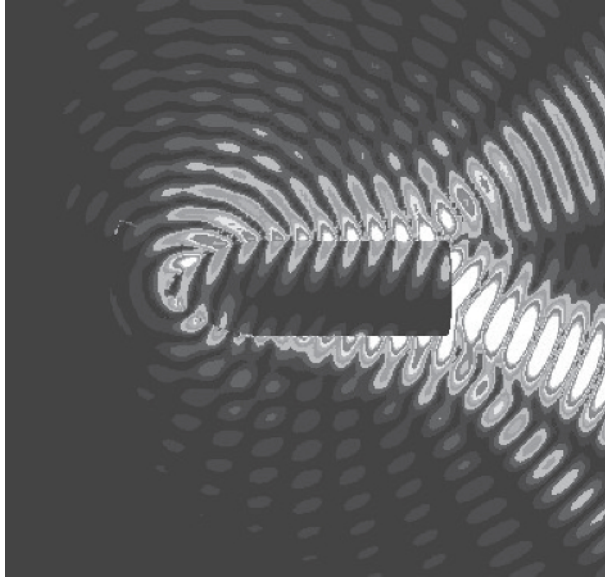


**FIGURE 6-8** ■ Time snapshot of the scattered field from a PEC ogive-cylinder illuminated 20 degrees up from the axis with  $E$  in the plane of the figure. Also shown are the instantaneous surface currents producing this scattered field.

cylinder (angle of reflection equal to angle of incidence). An ogive tip diffracted field radiating spherically from the front can be observed as well.

## 6.3 | RADAR CROSS SECTION DEFINITION

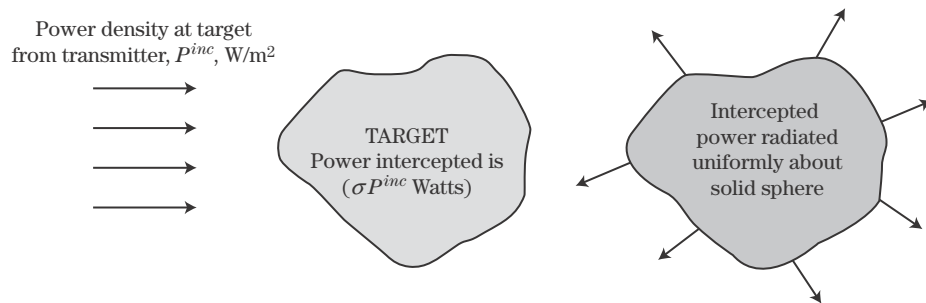
Radar cross section is a measure of power scattered in a given spatial direction when a target is illuminated by an incident wave. Another term for RCS is echo area. RCS is intended to characterize the target and not the effects of transmitter power, receiver sensitivity, and the distance or location between a target and the transmitter or receiver. Therefore, RCS is normalized to the power density of the incident wave *at the target* so that it does not depend on the distance from the illumination source to the target. This removes the effects of the transmitter power level and target distance. RCS is also normalized so that the inverse square falloff of scattered intensity back toward a receiver due to spherical spreading is not a factor; therefore, it is not necessary to know the position of the receiver.

### 6.3.1 IEEE RCS Definition

The Institute of Electrical and Electronics Engineers (IEEE) dictionary of electrical and electronics terms [4] defines RCS as a measure of the reflective strength of a target. Mathematically, it is defined as  $4\pi$  times the ratio of the power per unit solid angle scattered in a specified direction to the power per unit area in a plane wave incident on the scatterer from a specified direction. More precisely, it is the limit of that ratio as the distance from the scatterer to the point where the scattered power is measured approaches infinity,

$$\sigma = \lim_{R \rightarrow \infty} 4\pi R^2 \frac{|E^{scat}|^2}{|E^{inc}|^2} \quad (6.9)$$

**FIGURE 6-9 ■**  
Intuitive derivation of  
radar cross section  
[1].



where  $E^{scat}$  is the scattered electric field, and  $E^{inc}$  is the field incident *at the target*. Three cases are distinguished: (1) monostatic or backscatter; (2) forward scattering; and (3) bistatic scattering.

A formal cross section may also be defined for the energy that is scattered, absorbed, or removed from the incident wave. A total cross section can also be defined that includes all of these effects. The scattered energy is of greatest practical interest because it represents the energy available for radar detection.

### 6.3.2 Intuitive Derivation for Scattering Cross Section

The formal IEEE definition for RCS given in equation (6.9) can be made more plausible by considering the following derivation (Figure 6-9). Let the incident power density at a scattering target from a distant radar be  $P^{inc}$  W/m<sup>2</sup>. Considering the density at the target automatically removes from the definition transmitter power and the  $1/R^2$  intensity falloff. The amount of power intercepted by the target is then related to its cross section  $\sigma$ , with units of area, so that the intercepted power is  $\sigma P^{inc}$  W. This intercepted power is then either reradiated as the scattered power or absorbed as heat. Assume for now that it is reradiated as scattered power uniformly in all  $4\pi$  sr of space so that the scattered power density is given by

$$P^{scat} = \frac{\sigma P^{inc}}{4\pi R^2} \quad \text{W/m}^2 \quad (6.10)$$

Equation (6.10) is then solved for  $\sigma$ , assuming that the distance  $R$  is far from the target to avoid near-field effects:

$$\sigma = \lim_{R \rightarrow \infty} 4\pi R^2 \frac{P^{scat}}{P^{inc}} \quad (6.11)$$

RCS is therefore fundamentally a ratio of scattered power density to incident power density. The power or intensity of an EM wave is proportional to the square of its electric or magnetic field magnitude, so RCS can be expressed as

$$\sigma = \lim_{R \rightarrow \infty} 4\pi R^2 \frac{|E^{scat}|^2}{|E^{inc}|^2} = \lim_{R \rightarrow \infty} 4\pi R^2 \frac{|H^{scat}|^2}{|H^{inc}|^2} \quad (6.12)$$

because in the far field  $E$  and  $H$  are related to each other by the impedance of free space. The units for radar cross section  $\sigma$  is area, usually square meters. RCS is sometimes made nondimensional by dividing by wavelength squared,  $\sigma/\lambda^2$ .

This definition is made more recognizable by examining the basic radar range equation for power received by the radar,  $P_r$ , in terms of transmitted, scattered, and received power:

$$P_r = \frac{(P_t G_t / 4\pi R^2) \sigma}{4\pi R^2} A_r \quad (6.13)$$

The term in parentheses in the numerator is the power density at the target location (measured in  $\text{W/m}^2$ ). This incident power flux is multiplied by a cross section (area) and represents power captured from the incident wave and then reradiated by the target, some of which goes back toward the receiver. When this is divided by the return path spherical spreading factor, it gives the power density at the receiver for capture by the receiving antenna effective area,  $A_r$ .

The radar cross section of a target is a function of several attributes of the target, the radar observing the target, and the radar-target geometry. Specifically, RCS depends on the following:

- Target geometry and material composition.
- Position of transmitter relative to target.
- Position of receiver relative to target.
- Frequency or wavelength.
- Transmitter polarization.
- Receiver polarization.

When the transmitter and receiver are at different locations (Figure 6-10), the RCS is referred to as the bistatic radar cross section. In this case, the angular location of target relative to transmitter and receiver must be specified to fully specify the RCS. Monostatic or backscatter cross section is the usual case of interest for most radar systems. In this configuration the receiver and transmitter are collocated, often using the same antenna for transmitting and receiving (Figure 6-10). In this case only one set of angular coordinates is needed. Most experimental measurements are of backscatter cross section. Analytical RCS predictions, however, are much easier to make for bistatic cross section, with the illumination source fixed and the receiver position moved.

The radar cross section of a target may also be a function of the pulse width,  $\tau$ , of the incident radiation. In the usual radar case with microsecond pulse widths, the pulse is large enough such that the pulse illuminates the entire target at once (target length assumed much less than 1,000 feet in length). This condition, which is loosely equivalent to the

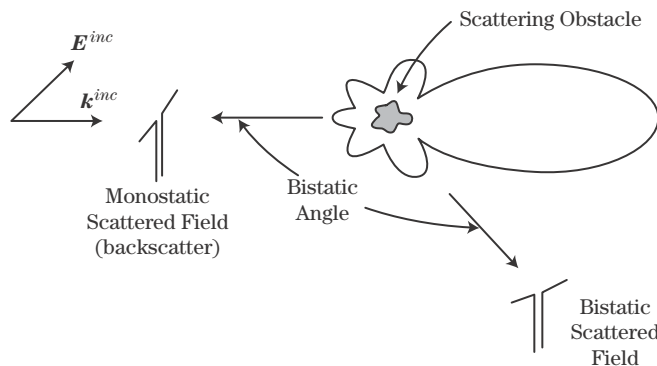


**FIGURE 6-10 ■**  
Monostatic or  
bistatic target cross  
section cases.

target being illuminated by a continuous wave (CW) at a specific frequency, is known as long-pulse illumination. In this case, all scattering mechanisms from the target add coherently to give the net reflected signal. When short pulses are used (large bandwidth), such as nanosecond pulses with spatial extents of only several feet, then each scatterer on the target contributes independently to the return signal in time. In this case the RCS is a collection of individual scattering returns separated in time. Short-pulse radars (or their wide bandwidth pulse compression waveform equivalents; see Chapter 20) are often used to identify these scattering centers on complex targets.

### 6.3.3 RCS Customary Notation

The units for radar cross section are square meters. However, the RCS of a target does not necessarily relate to the physical size of that target. Although it is generally true that larger physical targets have larger radar cross sections (e.g., the optical front face reflection for a sphere is proportional to its projected area,  $\sigma_{\text{sphere}} = \pi a^2$ ), not all RCS scattering mechanisms are related to size. Typical values of RCS can span  $10^{-5} \text{ m}^2$  for insects to  $10^{+6} \text{ m}^2$  for large ships. Due to the large dynamic range, a logarithmic power scale is most often used with the reference value of  $\sigma_{\text{ref}} = 1 \text{ m}^2$ :

$$\sigma(\text{dBsm}) = \sigma(\text{dBm}^2) = 10 \log_{10} \left( \frac{\sigma}{\sigma_{\text{ref}}} \right) = 10 \log_{10}(\sigma) \quad (6.14)$$

Both the notations  $\text{dBm}^2$  and  $\text{dBsm}$  are often used.

### 6.3.4 Polarization Scattering Matrix

#### 6.3.4.1 Scattering Matrix for Linear Polarization

Radar cross section, as a scalar number, is a function of the polarization of the incident and received wave. A more complete description of the interaction of the incident wave and the target is given by the polarization scattering matrix (PSM), which relates the scattered electric field vector  $\mathbf{E}^{\text{scat}}$  to the incident field vector  $\mathbf{E}^{\text{inc}}$ , component by component. In matrix notation, this is

$$\mathbf{E}^{\text{scat}} = \mathbf{S} \cdot \mathbf{E}^{\text{inc}} \quad (6.15)$$

$\mathbf{E}$  can be decomposed into two orthogonal directions or polarizations (because there is no component in the direction of propagation  $\mathbf{k}$ ); thus, the polarization scattering matrix,  $\mathbf{S}$ , is a  $2 \times 2$  complex matrix:

$$\mathbf{E}^{\text{scat}} = \begin{bmatrix} \mathbf{E}_V^{\text{scat}} \\ \mathbf{E}_H^{\text{scat}} \end{bmatrix} = \begin{bmatrix} S_{VV} & S_{VH} \\ S_{HV} & S_{HH} \end{bmatrix} \mathbf{E}^{\text{inc}} = \begin{bmatrix} S_{VV} & S_{VH} \\ S_{HV} & S_{HH} \end{bmatrix} \begin{bmatrix} \mathbf{E}_V^{\text{inc}} \\ \mathbf{E}_H^{\text{inc}} \end{bmatrix} \quad (6.16)$$

where  $\mathbf{E}^{\text{scat}}$  and  $\mathbf{E}^{\text{inc}}$  are the scattered and incident fields.  $\mathbf{E}_H^{\text{scat}}$  and  $\mathbf{E}_V^{\text{scat}}$  are the orthogonal vector vertical and horizontal polarization components of  $\mathbf{E}^{\text{scat}}$ , while  $\mathbf{E}_H^{\text{inc}}$  and  $\mathbf{E}_V^{\text{inc}}$  are the orthogonal vector vertical and horizontal polarization components of  $\mathbf{E}^{\text{inc}}$ .

The four complex elements of  $\mathbf{S}$  that specify the scattering matrix represent eight scalar quantities, four amplitudes and four phases. One phase angle is arbitrary and is used as a reference for the other three. If the radar system is monostatic (backscatter), then  $S_{VH} = S_{HV}$ , and  $\mathbf{S}$  can be specified by five quantities.

When a coherent radar that transmits and receives two orthogonal polarizations is present, the scattering matrix is determined for a given aspect angle at the radar frequency,  $f$ .

For a given target, aspect angle, and frequency, no more signal information can be extracted than what is contained in the scattering matrix for a narrow bandwidth pulse.

### 6.3.4.2 Scattering Matrix for Circular Polarization

In circular polarization, the electric field vector rotates in the plane perpendicular to the direction of propagation. The two orthogonal components of the electric field are called the *right-handed circular* and *left-handed circular* components (or just *right circular* [RC] and *left circular* [LC]). Consider an observer viewing a circularly polarized EM wave along the direction of propagation, and assume the wave is propagating away from the observer. This corresponds to considering the transmitted EM wave. The IEEE defines the case where the electric field vector rotates clockwise when viewed in this manner as RC rotation and the case where it rotates counterclockwise as LC rotation (Figure 6-11).

It follows that the apparent direction of rotation for a given circular polarization component is reversed for an incoming wave. To an observer viewing an incoming RC polarized wave, the electric field vector will appear to be rotating counterclockwise, while that of an incoming LC polarized wave will appear to be rotating clockwise.

Linear polarization can be transformed into circular polarization by shifting the phase of one of the two linear components by  $\pm 90$  degrees. The choice between right- and left-handed circular is determined by the sign of the phase shift. Specifically, the RC and LC components of an electric field vector can be derived from the horizontal and vertical components according to [2]:

$$\begin{bmatrix} E_{RC}^t \\ E_{LC}^t \end{bmatrix} = \frac{1}{\sqrt{2}} \begin{bmatrix} 1+j \\ 1-j \end{bmatrix} \begin{bmatrix} E_{HH}^t \\ E_{VV}^t \end{bmatrix} \quad (6.17)$$

where the superscript  $t$  indicates the transmitted field components. The inverse transform to obtain linear polarization components from circular components is

$$\begin{bmatrix} E_{HH}^t \\ E_{VV}^t \end{bmatrix} = \frac{1}{\sqrt{2}} \begin{bmatrix} 1 & 1 \\ -j & j \end{bmatrix} \begin{bmatrix} E_{RC}^t \\ E_{LC}^t \end{bmatrix} \quad (6.18)$$

as may be verified by taking the matrix inverse of the transformation matrix in equation (6.17).

Received polarization can be defined in a similar manner. The LC and RC definitions change because the observer is now looking in the direction of propagation, which is from

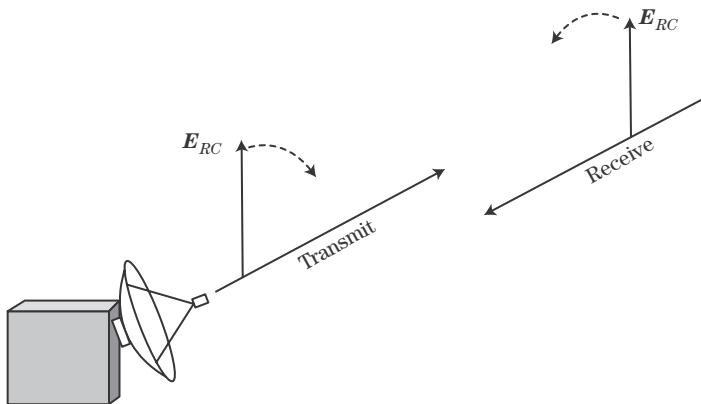


**FIGURE 6-11** ■ Circular polarization sense, CCW or CW, is referenced by looking in the direction of propagation  $k$  [1].

the target toward the receiver, while the radar system has defined LC and RC as viewed from the radar to the target. Therefore, with the superscript  $r$  denoting received field components,

$$\begin{bmatrix} E_{RC}^r \\ E_{LC}^r \end{bmatrix} = \frac{1}{\sqrt{2}} \begin{bmatrix} 1-j \\ 1+j \end{bmatrix} \begin{bmatrix} E_{HH}^t \\ E_{VV}^t \end{bmatrix} \quad (6.19)$$

which is seen to be the complex conjugate of the transmitted case (6.17).

The circular polarization PSM contains no more information than the linear polarization PSM. If a linear PSM has been computed or measured, the corresponding circular PSM can be obtained by using equations (6.17) through (6.19) to obtain [2]

$$\begin{bmatrix} S_{LL} & S_{LR} \\ S_{RL} & S_{RR} \end{bmatrix} = \frac{1}{2} \begin{bmatrix} 1-j \\ 1+j \end{bmatrix} \begin{bmatrix} S_{HH} & S_{HV} \\ S_{VH} & S_{VV} \end{bmatrix} \begin{bmatrix} 1 & 1 \\ -j & +j \end{bmatrix} \quad (6.20)$$

where subscripts  $L$  and  $R$  indicate left and right circular polarization.

A characteristic feature of circular polarization is that single- or odd-bounced scattering changes the sense of the polarization, from LC to RC or from RC to LC. For linear polarization single-bounce specular scattering, the scattered energy has the same polarization as the incident polarization. This occurs because the scattered field is phase-shifted by 180 degrees relative to the incident field—that is, in the opposite direction (reflection coefficient  $\Gamma = -1$ ).

## 6.4 | THREE SCATTERING REGIMES

Scattering mechanisms depend on scattering body size,  $L$ , relative to wavelength,  $\lambda$ . When  $\lambda$  is much larger than the body size, scattering is due to induced dipole moments; when  $\lambda$  is approximately the same as body size, surface wave effects such as edge, traveling, and creeping waves along with optical effects are important. When  $\lambda$  is much smaller than body size, surface wave effects become insignificant, and only optical effects are important.

The three scattering regimes are as follows:

Rayleigh	$\lambda \gg L$	Dipole-like scattering
Resonant	$\lambda \approx L$	Optics scattering + traveling, edge, and creeping surface waves
High frequency	$\lambda \ll L$	Optics scattering: angle of incidence = angle of reflection, end region, edge diffraction, multiple bounce

The classic illustration of radar cross section over these three regimes is that of a sphere as shown in Figure 6-12, where  $\sigma$  has been normalized to the projected area of the sphere,  $\pi a^2$ , plotted as a function of sphere circumference normalized to wavelength,  $ka = 2\pi a/\lambda$ . Figure 6-12 is a log-log plot over four orders of magnitude in  $\sigma$  and three orders of magnitude in sphere circumference. When the wavelength is much greater than the sphere circumference, the sphere's RCS is proportional to  $a^2(ka)^4$ . Although  $\sigma$  is small in this regime, it increases as the fourth power of frequency and sixth power of radius. When the circumference is between 1 and 10 wavelengths, the RCS exhibits an oscillatory behavior due to the interference of the front face optics specular return and the two surface creeping waves that propagate around the back of the sphere, as implied by the small sphere shown in the middle of Figure 6-12. This range of wavelengths is known as the resonant region. When the sphere's circumference is large compared with wavelength, the creeping waves

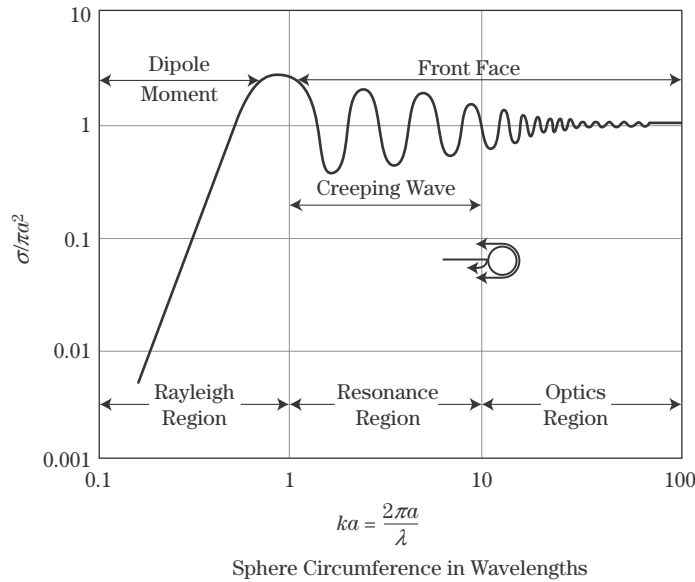


**FIGURE 6-12** ■ Sphere scattering from Rayleigh, resonance, and optics regions, [1].

die out before they can radiate back toward the radar, the oscillatory behavior decays, and only the optics front face reflection is left, which for a double-curved surface is  $\sigma = \pi a^2$ , the projected area of the sphere. This is the optics region.

### 6.4.1 Rayleigh Region Dipole Scattering

When the incident wavelength,  $\lambda$ , is much greater than body size,  $L$ , scattering is called Rayleigh scattering, after Lord Rayleigh's analysis of why the sky is blue: the shorter blue wavelengths are more strongly scattered than the longer red wavelengths.

In the Rayleigh region, also called the low-frequency case, there is essentially little phase variation of the incident wave over the spatial extent of the scattering body: each part of the body “sees” the same incident field at each instant of time. This situation is equivalent to a static field problem, except that now the incident field is changing in time. This quasi-static field builds up opposite charges at the ends of the body; in effect, the incident field induces a dipole moment. The strength of this dipole is a function of the size and orientation of the body relative to the vector direction of the incident field. Dipole moments are defined as charge density multiplied by separation distance. The salient characteristic of Rayleigh scattering is that cross section is proportional to the fourth power of the frequency or wave number [5]:

$$\sigma \propto \omega^4 \quad \text{or} \quad k^4 \quad (6.21)$$

The low-frequency approach can be used until there is appreciable phase change of the incident wave over the length of the scatterer.

### 6.4.2 Resonant Region Scattering

When the incident wavelength is on the order of the body size, the phase of the incident wave changes significantly over the length of the scattering body (Figure 6-12). Although there are no absolute definitions, the resonant region is typically taken to be the range of wavelengths such that the target body is between  $\lambda$  and  $10\lambda$  in size,  $1 < L/\lambda < 10$ . This region has two classes of scattering mechanisms: (1) optical, with the local angle of



reflection equal to the angle of incidence; and (2) surface wave effects, where nonlocal regions interact.

Surface wave scattering mechanisms are distinctly different from optical scattering mechanisms. The name *resonant region* is a bit of a misnomer in that these mechanisms are not from high-quality factor sharply resonant phenomena. Rather, the physical mechanisms are due to EM energy that stays attached to the body surface. Surface wave types are *traveling*, *edge*, and *creeping*. Surface wave backscatter occurs when this surface energy is reflected from some aft body discontinuity or, as in the case of a creeping wave, when the energy flow is completely around the body.

Surface wave scattering is independent of body size. Cross section magnitudes are proportional to wavelength squared—that is,  $L^0\lambda^2$ . From this relation it can be seen why surface wave effects are important for resonant region body sizes. Surface wave effects are present in the optics region, but because of the smaller wavelengths the scattering magnitudes are much smaller than optical region scattering magnitudes, which most often are proportional to one of the following:  $L\lambda$ ,  $L^2\lambda^0$ ,  $L^3\lambda^{-1}$ , or  $L^4\lambda^{-2}$ .

Resonant region scattering mechanisms are typically due to one region of the scattering body interacting with another region. Thus, edge waves involve an entire edge in front of an edge termination aft discontinuity, surface waves over much of the entire surface in front of the surface termination aft discontinuity, and creeping waves over the shadowed regions. Overall geometry is important; however, small-scale details (relative to wavelength) are not.

### 6.4.3 High-Frequency Optics Region

When the wavelength becomes much smaller than the body size,  $\lambda \ll L$ , a localized scattering center approach can be used to represent the scattering physics; that is, local effects are more important than collective body–body interactions. In this region, collective surface edge, traveling, and creeping wave effects are very weak, so the body is now treated as a collection of independent scattering centers. Detailed geometries now become important in the scattering process, and net scattering from the body is the complex phasor sum of all the individual scattering centers.

True optics scattering is defined in the limit as  $\lambda \rightarrow 0$ . For most cases of microwave interest, finite body size effects must still be dealt with.

Optical regime scattering mechanisms are as follows:

- *Specular scattering*: This is true optics scattering in the sense of  $\lambda \rightarrow 0$ . Ray optics, where angle of reflection is equal to angle of incidence, apply. Scattering is analogous to mirror reflections in optics and is responsible for bright spike-like scattering.
- *End-region scattering*: This is scattering from the end regions of finite bodies. It produces the *sidelobes* in directions away from the direction of specular scattering. End-region sources arise from the rapid truncation of surface currents at body ends.
- *Diffraction*: This is end-region scattering in the specular direction due to edge-induced currents at leading or trailing edges, tips, or body regions of rapid curvature change.
- *Multiple bounce*: This is the separate case of mutual body interaction in the sense that one body surface specularly scatters energy to another body surface, which reflects that energy back to the observer (e.g., corner reflectors and cavities).

**TABLE 6-1** ■ Scattering Mechanism and Relevant Scattering Regime

Scattering Mechanisms	Scattering Regime	Comments
Dipole	Dipole	Small scattering varies as the fourth power of frequency and the sixth power of size.
Surface waves	Resonance	Traveling, edge, and creeping waves; grazing angle phenomena; depends on polarization
Specular	Optics, resonance	Angle of reflection = angle of incidence for planar, single-, and double-curved surfaces
Multiple bounce	Optics, resonance	Few bounces (e.g., corner); many bounces (e.g., cavities)
End region	Optics, resonance	Sidelobes of a plate or cylinder from the ends of the surface
Edge diffraction	Optics, resonance	Diffraction in the specular direction; depends on polarization
Discontinuities, gaps, cracks	Optics	Surface imperfections important at higher frequencies

Table 6-1 lists the various scattering mechanisms and the scattering regimes where they apply.

## 6.5 | HIGH-FREQUENCY SCATTERING

High-frequency scattering is defined as the case when the wavelength,  $\lambda$ , is much smaller than body size. Scattering centers are now typically local regions on the body and are referred to as scattering centers.

### 6.5.1 Phasor Addition

There is almost always more than one scattering center in view for any given aspect angle. The overall or net scattering is then the coherent phasor sum of all the scattering mechanisms from individual centers. The coherent phasor sum is the complex vector addition of scattering amplitudes depending on their electrical phase (path length measured in wavelengths) according to

$$\mathbf{k} \cdot \mathbf{R} = 2\pi \left( \frac{R}{\lambda} \right) \quad (6.22)$$

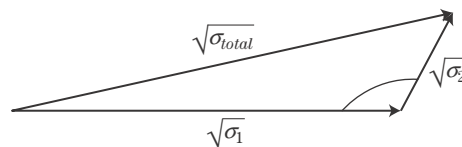
where distance,  $R$ , is the total two-way distance from the transmitter to the target scattering center and back to the receiver. Specifically, the total coherent RCS from  $N$  scattering centers active at a given viewing angle is

$$\sigma_{total} = \left| \sum_{i=1}^N \sqrt{\sigma_i} e^{j2\mathbf{k} \cdot \mathbf{R}_i} \right|^2 \quad (6.23)$$

where  $\sqrt{\sigma_i}$  and  $\mathbf{R}_i$  are the amplitude and spatial position of each individual scattering center. This sum depends on relative spatial position (i.e., spatial phase) of each contributor as well as its amplitude. The factor of two in the phase term results from the fact that the

**FIGURE 6-13 ■**

Total scattering is the phase sum of individual scattering centers.



total distance from transmitter to target and back to receiver is twice the one-way distance. The coherent phasor sum is analogous to force vector addition in kinematics.

To illustrate, consider just two scattering centers,  $\sigma_1$  and  $\sigma_2$ , with voltage amplitudes proportional to  $\sqrt{\sigma_1}$  and  $\sqrt{\sigma_2}$ , and let  $\sqrt{\sigma_{total}}$  be the amplitude of the phasor sum of the electric fields produced by these two scattering mechanisms. The coherent phasor sum (Figure 6-13) depends not only on the amplitude of the two scattering centers but also on their relative phase.

Figure 6-14 shows how the RCS of two individual point scatterers add and subtract to create different values of total RCS depending on their relative sizes and spatial phase. Point scatterers have no angular dependence, so the only source of phase differences is differences in their spatial location. Let the point scatterers lie on some baseline and be spaced  $2\lambda$  apart. Now consider three cases.

In case 1, both scatterers have the same RCS,  $\sigma_1 = \sigma_2 = 1 \text{ m}^2 = 0 \text{ dBsm}$ . Figure 6-14a illustrates the coherent phasor sum RCS in the plane of the two scattering centers. When the transmitter/receiver is on a line perpendicular to the baseline, the distance to each scattering center is the same, so the two complex amplitudes add in phase to give  $(\sqrt{1} + \sqrt{1})^2 = 4 \text{ m}^2 = 6 \text{ dBsm}$  for the total RCS. When the transmitter/receiver is collinear with the baseline, the round-trip distance difference is  $4\lambda$ , so again the complex amplitudes of the two scatterers add in phase to give a total RCS of 6 dBsm. At selected angular locations in between, the spatial phase difference becomes 180 degrees, and the two scatterers add out of phase. Since they are equal-RCS scatterers, the net RCS is zero, and the null depths are infinitely deep on the logarithmic dBsm scale.

In case 2, shown in Figure 6-14b, the radar cross sections of the two scatterers differ in magnitude by a factor of four,  $\sigma_1 = 1 \text{ m}^2 = 0 \text{ dBsm}$  and  $\sigma_2 = 0.25 \text{ m}^2 = -6 \text{ dBsm}$ . As before, when the receiver is on a line perpendicular to the baseline, the distance to each scattering center is the same, and the individual voltages add in phase to give

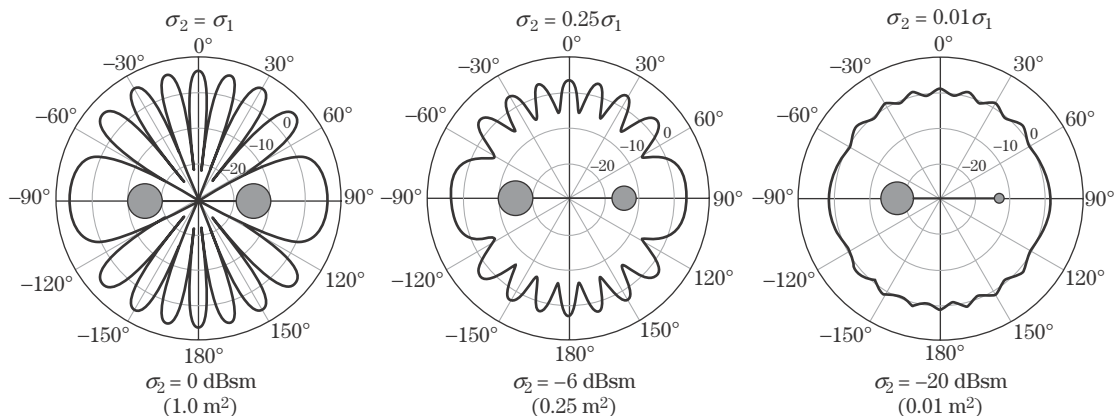


**FIGURE 6-14 ■** Phase sum of two point scattering centers of different magnitudes. Scale: dBsm, 10 dB/div.

$(\sqrt{1} + \sqrt{1/4})^2 = 2.25 \text{ m}^2 = 3.52 \text{ dBsm}$ . When the transmitter/receiver is collinear with the baseline, the round-trip distance difference is  $4\lambda$ , so again the two scatterers add in phase to 3.52 dBsm. At angles where the two spatial phases are 180 degrees apart, the scatterers add out of phase to give  $(\sqrt{1} - \sqrt{1/4})^2 = 0.25 \text{ m}^2 = -6.0 \text{ dBsm}$  for the null depths.

In case 3 (Figure 6-14c), the two scatterers differ in magnitude by a factor of 100,  $\sigma_1 = 1 \text{ m}^2 = 0 \text{ dBsm}$  and  $\sigma_2 = 0.01 \text{ m}^2 = -20 \text{ dBsm}$ . As before, when the receiver is on a line perpendicular to the baseline or is collinear with the baseline, the two scatterers add in phase to give  $(\sqrt{1} + \sqrt{1/100})^2 = 1.21 \text{ m}^2 = 0.83 \text{ dBsm}$ . At angles where the two spatial phases are 180 degrees apart, the scatterers phase subtract to give  $(\sqrt{1} - \sqrt{1/100})^2 = 0.81 \text{ m}^2 = -0.92 \text{ dBsm}$  for the null depths.

From these results it is seen that the interaction of two equal or nearly equal RCS scatterers can be up to four times, or 6 dB, higher than that of a single scattering center when they add in phase, and that when they subtract, the null depths can be very deep. However, when two scatterers of significantly different RCS interact, the lower-RCS scatterer does not contribute much to the net scattering on the dB scale.

## 6.5.2 Specular Scattering

Specular scattering from flat, single-curved, or double-curved surfaces is scattering where the angle of reflection is equal to the angle of incidence. In very simple terms, the reflected wave bounces like a billiard ball from the surface (Figure 6-15). Specular scattering is often of very high intensity. The target scattering center surface normal must point back toward the radar transmitter/receiver direction for specular scattering to occur in the backscatter direction.

A key notion in specular scattering is that of the *specular point*. This point is the surface location where the angle of incidence is equal to the angle of reflection. This location is also called the flash point, hot spot, or stationary phase point. In geometrical terms, this point determines the shortest distance between the transmitter and receiver for a location on the surface. This point is also the surface location for Fermat's minimum path length; that is, the path length is stationary with respect to variations in path. When the receiver and transmitter are collocated, as in backscatter, the specular points are those surface locations where the local normal points back toward the illuminating radar.

Figure 6-16 shows a bistatic configuration of transmitter and receiver. The surface specular point lies on a line between an image of the transmitter (below the surface) and the receiver or, equivalently, on a line between an image of the receiver and the transmitter. This line is the shortest distance between the transmitter and receiver via the surface. Currents in the vicinity of the specular point add in phase to create the high-magnitude flash in the specular direction. Currents outside this specular region add out of phase and do not contribute to the flash.

The occurrence of specular scattering is very dependent on the geometry of the scattering surface and the angles to the transmitter and receiver. A flat surface has only one backscatter specular point—that is, only one spatial direction where the surface normal

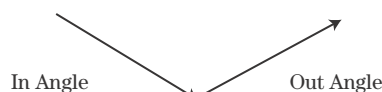
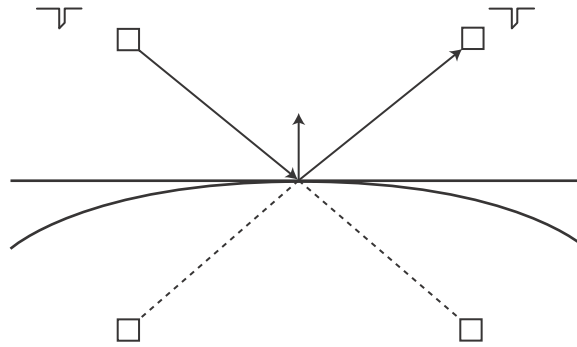


**FIGURE 6-15** ■  
Specular scattering,  
Snell's law.

**FIGURE 6-16 ■**  
Surface specular  
point for a bistatic  
radar.



can point back toward a radar. A sphere has an infinite number of specular points; that is, one is always perpendicular to the sphere surface regardless of view angle. A cylindrical surface has only one plane in space perpendicular to the surface where there is specular scattering.

Backscatter amplitude for specular scattering depends on the constant phase area,  $A_{cp}$ , at the specular point and on the wavelength,

$$\sigma_{\text{specular}} = 4\pi \frac{A_{cp}^2}{\lambda^2} \quad (6.24)$$

In the flat plate case, the constant phase area is the physical area of the plate. In this case all elementary regions of the plate are equidistant from the transmitter/receiver. Hence, all of these elemental areas add in phase to give the large net specular amplitude.

The double-curved surface constant phase area depends on the two radii of curvature at the specular point. As the incident wave passes over the surface, only the currents in a small region about the specular point can add in phase to the receiver/transmitter. The sharper the curvatures (smaller radii of curvature), the smaller the constant phase area dimension,  $L_{cp}$ :

$$L_{cp} \propto \sqrt{\frac{R_c \lambda}{2}} \quad (6.25)$$

For double-curved surface backscatter, the two constant phase dimensions correspond to the curvature of the surface at the specular point. The RCS is

$$\sigma = \pi R_1 R_2 \quad (6.26)$$

where  $R_1$  and  $R_2$  are the two specular point surface radii of curvature. Equation (6.26) is a very simple result that depends only on geometric curvature parameters and not on wavelength. As an example, the RCS of a prolate spheroid when viewed from the small end is less than when viewed from broadside due to the difference in the radii of curvature with the change in the position of the specular point.

In the cylindrical case, the surface has only one radius of curvature for the constant phase dimension, with the other dimension determined by cylindrical length. Cylindrical RCS becomes

$$\sigma_{cyl} = \frac{2\pi}{\lambda} R L^2 = k R L^2 \quad (6.27)$$

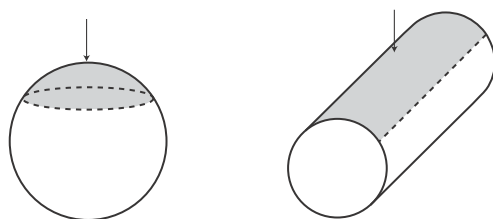


**FIGURE 6-17** ■ Specular point constant phase current region for backscatter when viewed from the top.

Figure 6-17 shows spherical and cylindrical specular point areas when a backscatter radar is above the target.

### 6.5.3 End-Region Scattering

Currents at the ends of a surface have two types of scattering. One is called end-region scattering and is responsible for plate sidelobes. The second is edge diffraction and is due to local edge line sources. Even though they both occur at edges, the sources are fundamentally different. Each of these sources scatters energy into directions other than the specular direction of the surface.

End-region scattering occurs when surface currents do not taper smoothly to zero at an edge; rather, they abruptly change value. This abrupt change gives rise to a scattering center. This mechanism scatters energy into directions other than the specular direction. This is why the end-region sources are said to produce the sidelobes of the RCS pattern. End-region scattering does not depend on polarization.

Consider backscattering from a  $10\lambda$  flat plate when viewed perpendicular to one of its edges (Figure 6-18 and the left half of Figure 6-19). Each end region becomes a scattering center source, and they are of equal magnitude. Thus, they add in or out of phase to give the oscillatory sidelobe pattern away from the specular direction. As the radar moves toward a grazing aspect angle, the projected area of the plate ends decreases, so the amplitude of the sidelobes also decreases. The end-region “source” area is determined by its projected area relative to the wavelength. When viewed perpendicular to an edge, the linear plate dimension,  $L$ , determines the effective end region size.

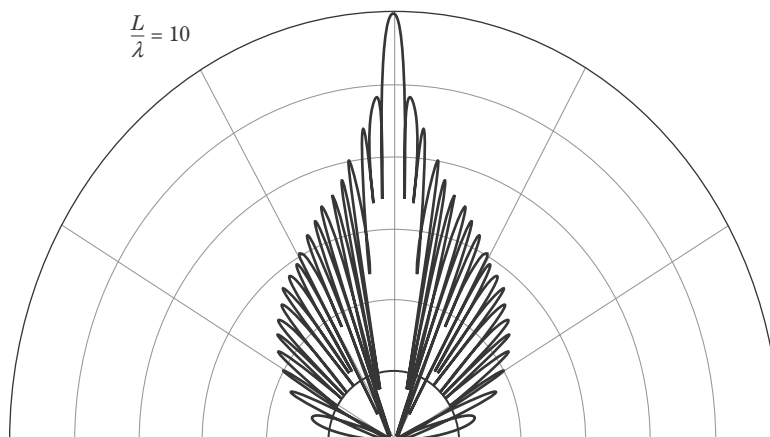
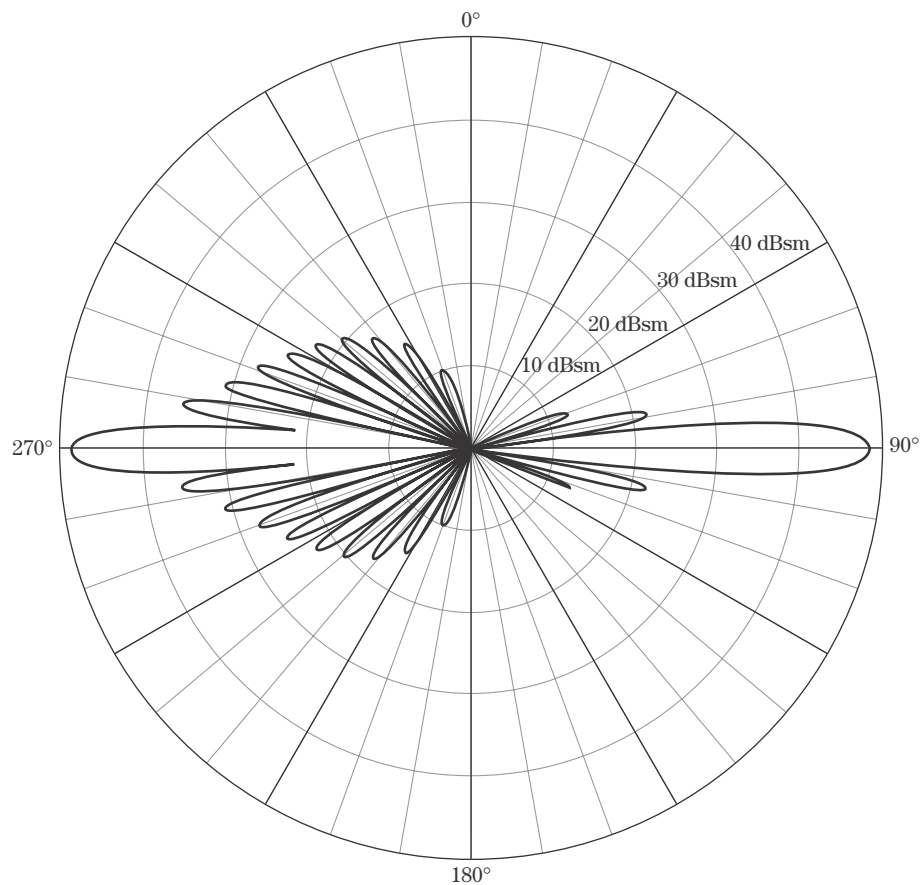


**FIGURE 6-18** ■ Backscatter from a flat plate when viewed perpendicular to an edge. The side lobes are due to the truncated end region currents phase adding/subtracting. The first side lobe is 13 dB down from specular. Scale is 10 dB/div.

**FIGURE 6-19 ■**  
 Plate backscatter showing end region side lobe scattering: Left) Viewed perpendicular to edges; Right) Viewed along diagonal.



The end-region source strengths for this plate change if the plate is viewed in a plane along its diagonal. In this case the end regions are the four corners of the plate. These areas are much smaller than the end-region area when the plate is viewed perpendicular to its edge; thus, the sidelobe pattern is much smaller (right half of Figure 6-19). In this case, the first sidelobe is 27 dB down from the specular peak, and the entire sidelobe pattern is much lower than when the plate is viewed perpendicular to its edges.

As further illustration of end-region sources, Figure 6-20 shows the RCS scattering centers of the plate when viewed at 45 degrees perpendicular to its edges. Two end-source regions are evident. When the plate is viewed at 45 degrees along its diagonal (Figure 6-21), four much smaller scattering center end regions are seen. Thus, in the diagonal view cut, sidelobes are much smaller since the end-region area sources are smaller.

#### 6.5.4 Edge Diffraction

Edge diffraction is due to induced localized line source (wire-like) currents at edges. Edge currents give rise to specular scattering on what is called the Keller cone of reflected rays and typically dominates grazing angle scattering (Figure 6-22).



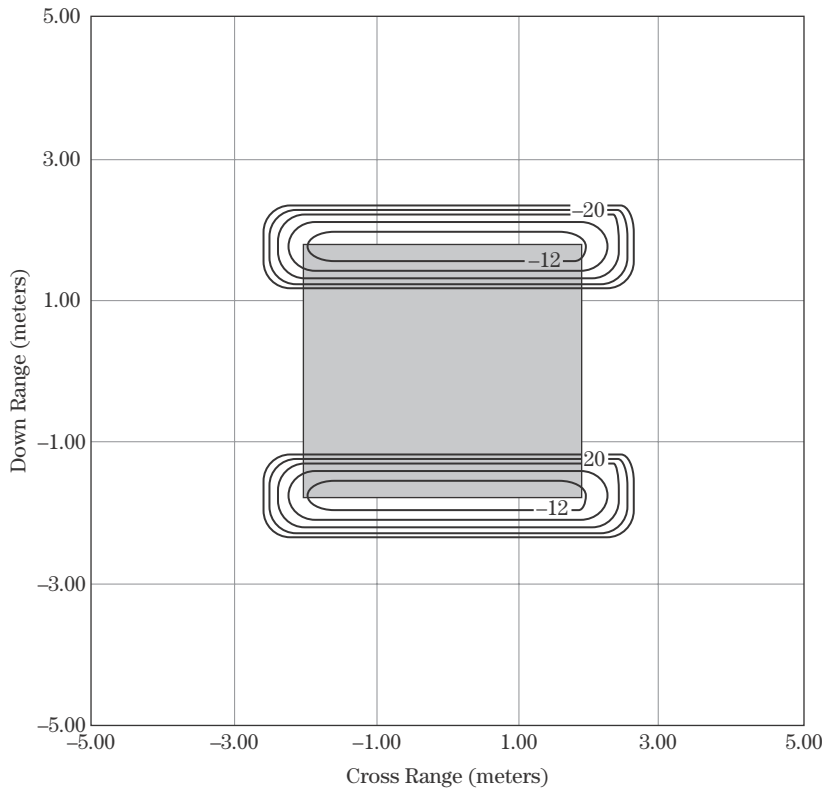


**FIGURE 6-20** ■ Flat-plate physical optics end-region return for oblique 45 degree backscatter looking perpendicular to edge of plate. These end regions produce the side lobes as they phase add or subtract. Image analytically computed using physical optics currents; that is, edge diffraction is not included, which at this angle is not yet significant. Plate size is  $5\lambda$ .

This “cone” of rays occurs due to cylindrical azimuthal symmetry of the local wire-like edge line source. Diffraction edge currents add in phase only in the specular direction, that is, on the Keller cone [6]. Every ray on this cone is in the specular direction. Edge normals are a disk of normal vectors perpendicular to the edge. The edge specular point is that point on the edge where the angle of reflection is equal to the angle of incidence.

When only backscatter is considered, the Keller cone degenerates into a disk of reflected radiation, and, in this case, the specular direction occurs only when the disk normal points back toward the radar. Thus, for backscatter, edge diffraction occurs only when the radar is perpendicular to an edge.

Edge diffraction depends on polarization (Figure 6-23). Two cases occur: (1) the incident electric field is parallel to the edge (leading-edge [LE] diffraction); and (2) the incident electric field is perpendicular to the edge (trailing-edge [TE] diffraction).<sup>1</sup>

The magnitude of edge diffraction has a weak dependence on the interior-included angle. A practical approximation for backscatter radar cross section for an edge of length  $L$  is

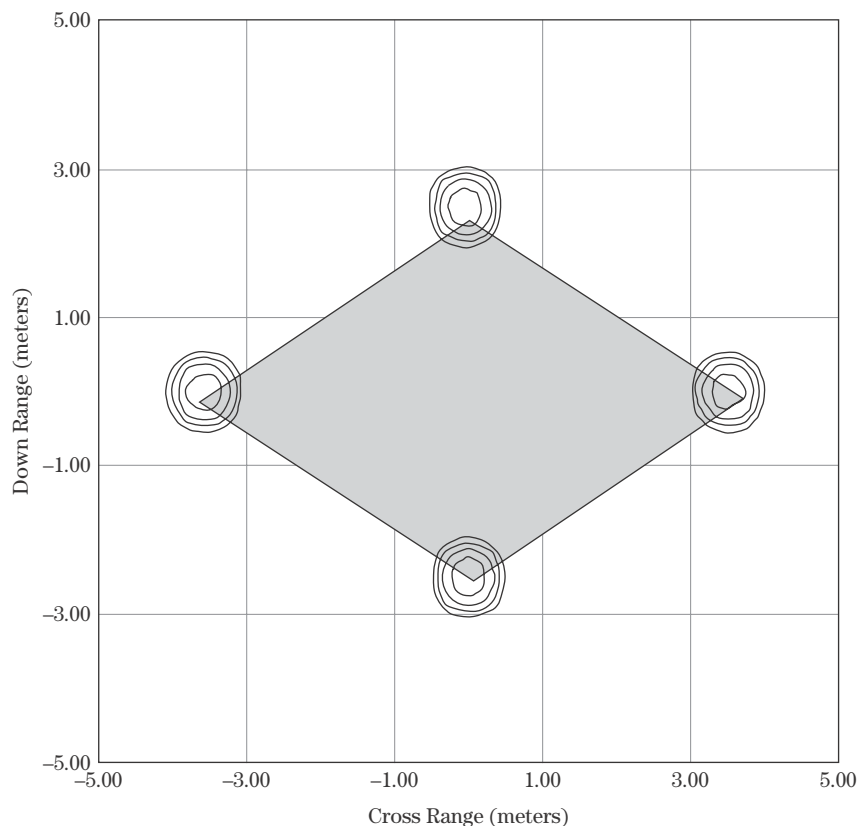
$$\sigma = \frac{L^2}{\pi} \quad (6.28)$$

which for a 1 ft. edge has a specular return of approximately  $-15$  dBsm.

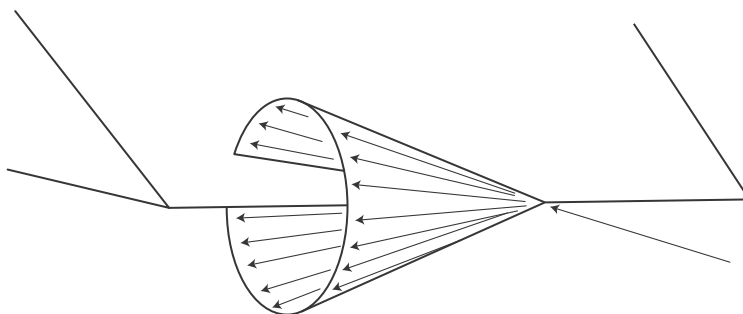
<sup>1</sup>This leading- and trailing-edge terminology is not to be confused with the LE and TE of airfoil surfaces.

**FIGURE 6-21 ■**

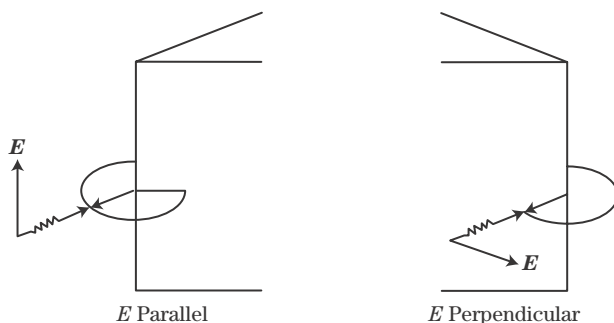
Flat-plate physical optics end-region return for oblique 45 degree incidence looking along diagonal of plate. These much smaller end regions produce lower side lobe envelopes as they phase add/subtract compared to looking perpendicular to an edge. Image analytically computed using physical optics current; that is, edge diffraction is not included, which at this angle is not yet significant. Plate size is  $5\lambda$ .

**FIGURE 6-22 ■**

Keller cone of edge specular reflected rays. Cone is due to symmetry of wire like local edge currents. Cone is the specular direction(s) of the incident ray, (from Knott [1]).

**FIGURE 6-23 ■**

Edge diffraction depends on polarization:  $E$  parallel or perpendicular to edge.



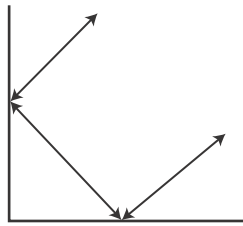


**FIGURE 6-24 ■**  
Multiple bounce is two or more specular scatters which reflect back to a radar.

### 6.5.5 Multiple-Bounce Scattering

Multiple-bounce scattering occurs when two or more specular bounces act in combination to reflect incident energy back to a receiver (Figure 6-24). Multiple-bounce scattering has two broad classes: one involving only a few specular bounces, such as a corner reflector; and the other involving many bounces such as a jet engine inlet/exhaust cavity of an aircraft. Multiple-bounce scatters are often characterized as having a high-level return over a wide angular region. This is why corner reflectors are often used as RCS augmenter devices on the masts of sailboats and why traditional ship construction, with many bulkheads and decks at right angles to each other and to the sea surface, produces vessels with rather large RCS.

The simplest corner reflectors are dihedrals and trihedrals formed by the intersection of two or three surfaces, respectively, intersecting at right angles. The RCS of a dihedral at X-band with square sides of dimension 17.9 cm is shown in Figure 6-25 [1]. Note the large central return over a wide angular region. The peaks at  $\pm 45$  degrees correspond to the single-bounce specular return from each of the two planar surfaces.

Another class of multiple-bounce geometries includes the jet engine inlet cavity of high-performance aircraft. This case is typically characterized by more than two bounces. Unless there is an energy absorption mechanism, a cavity that is open at only one location will reflect back all of the energy incident upon it. When numerous bounces occur, exit energy is often randomized in the exit direction.

Multiple-bounce geometries can also occur in cases where there is not an “obvious” corner reflector, such as an edge that is perpendicular to a single- or double-curved surface (Figure 6-26). Another example is a double-curved surface near any other target, such as a sphere in the vicinity of a planar surface (Figure 6-27).

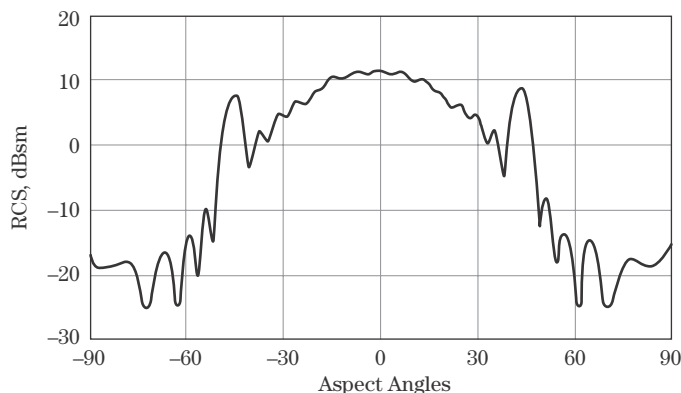


**FIGURE 6-25 ■**  
Multiple bounce dihedral backscatter showing a large central region of scattering [Knott, 1].

**FIGURE 6-26 ■**  
Multiple bounces  
can exist for a  
variety of geometric  
arrangements.

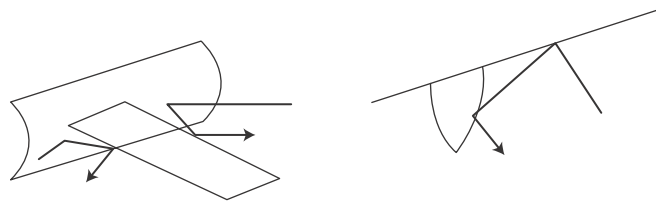
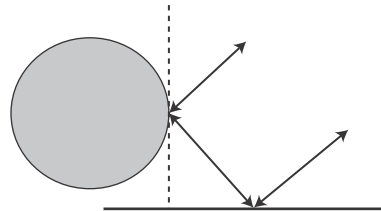


**FIGURE 6-27 ■**  
Doubly curved  
surfaces often form  
corner reflectors  
with other surfaces.



## 6.6 | EXAMPLES

This chapter concludes with RCS examples from a flat plate, an A7 aircraft at X-band, and a fictional geometry called a “stove pipe aircraft.” Far-field coherent patterns as well as scattering center images will be presented.

The backscattering from a flat plate when viewed perpendicularly to one of its edges exhibits three optics regime scattering mechanisms: specular, end region, and edge diffraction. Figure 6-28 [7] shows the measured RCS for a 6.5 inch square plate at X-band for both polarizations.

The specular spike occurs when the plate is viewed at 0 degrees, that is, perpendicular to the plate. This spike has the same amplitude, approximately 8.75 dBsm, for both polarizations. The null-to-null beamwidth, given by

$$\theta = 57 \frac{\lambda}{L} \text{ degrees} \quad (6.29)$$

where  $L$  is the plate dimension, is approximately 12 degrees. End-region scattering is dominant from the first null out to about 40 degrees. The in-phase or out-of-phase addition from the two equal area end regions creates this part of the RCS pattern. The sidelobes fall off as the end-region projected area becomes smaller (cosine function).

This part of the pattern is the same for both polarizations. Edge diffraction then dominates the pattern from 40 degrees out to grazing (approaching 90 degrees), now with distinctly different results for each polarization. The case of the electric field parallel to an edge (on the left side of the figure) has a value at grazing of  $-20$  dBsm, which is consistent with equation (6.28). The case where the electric field is perpendicular to an edge (right side of the figure) can better be characterized as a traveling wave return since the plate is only  $5\lambda$  in size.

A very complex backscatter example at X-band is that of an A7C Corsair aircraft as measured at the Navy’s Junction Ranch range in California. The test measurements were of a full-scale aircraft (Figure 6-29), where the vehicle is supported on a tapered low RCS Styrofoam column. The column is tapered so that its (small) specular cylinder return is not normal to the test radar. The tie-down ropes are also oriented so that they are not perpendicular to the test radar.

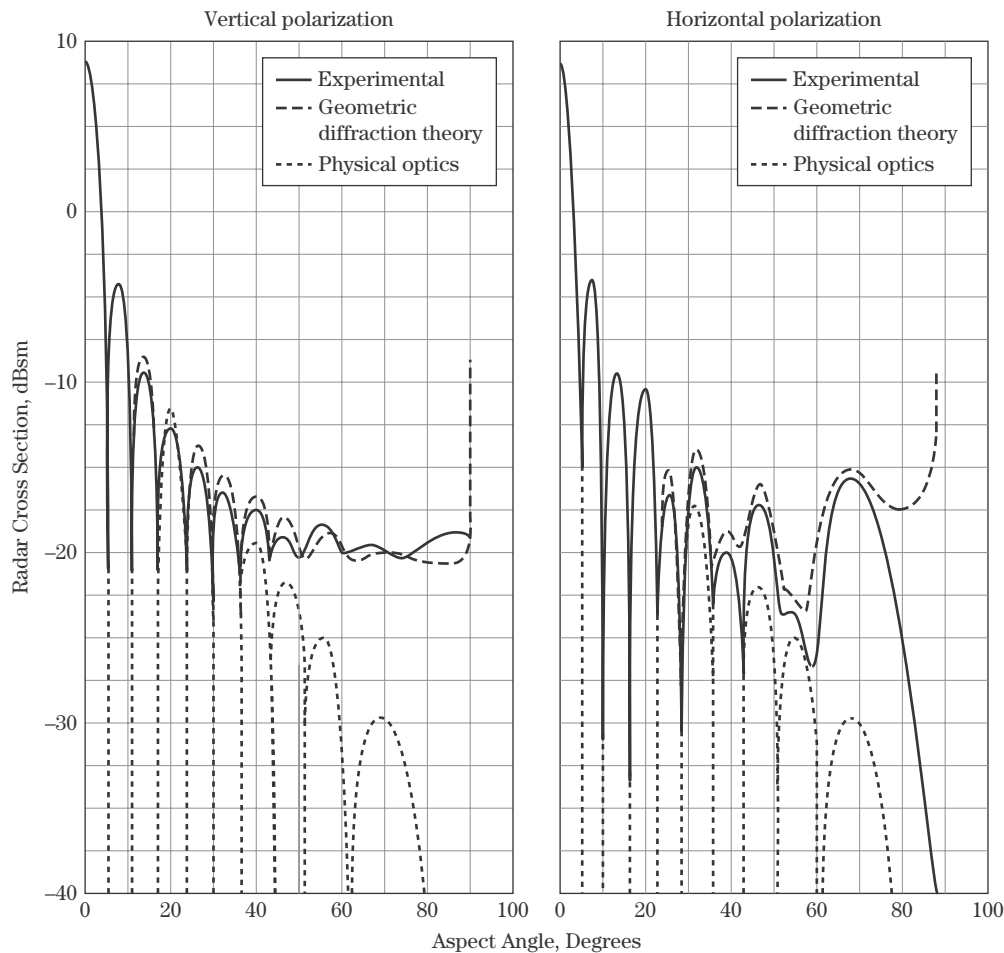
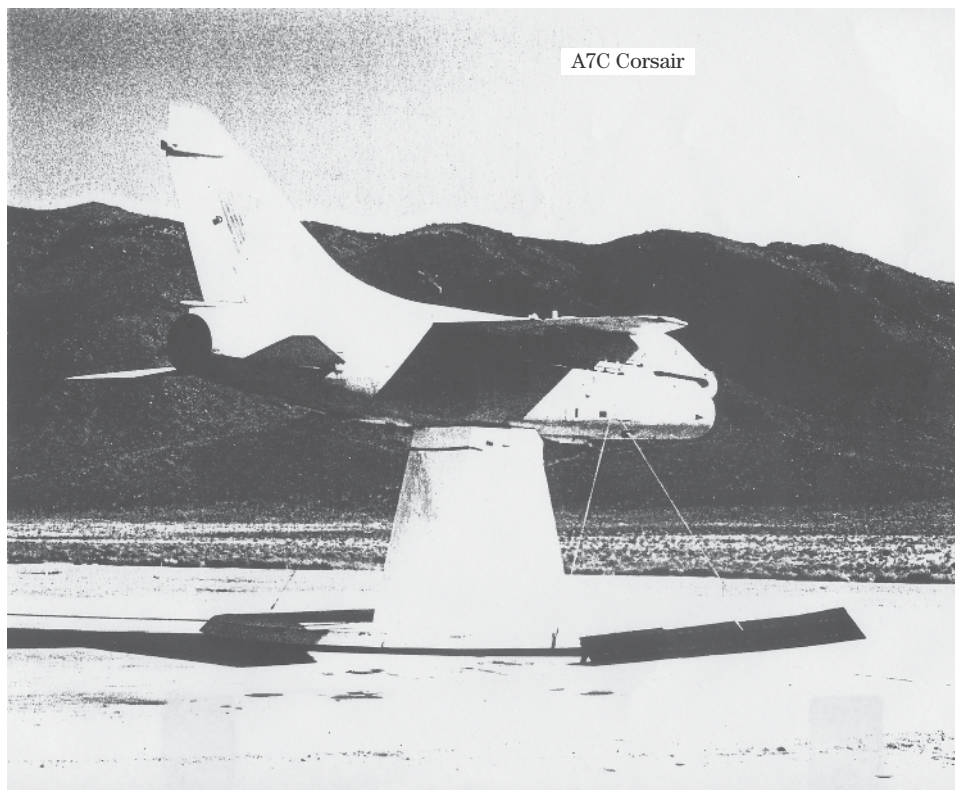


**FIGURE 6-28** ■ RCS patterns of a 6.5 in. square plate at a wavelength of 1.28 inches viewed perpendicular to its edges [from 7].

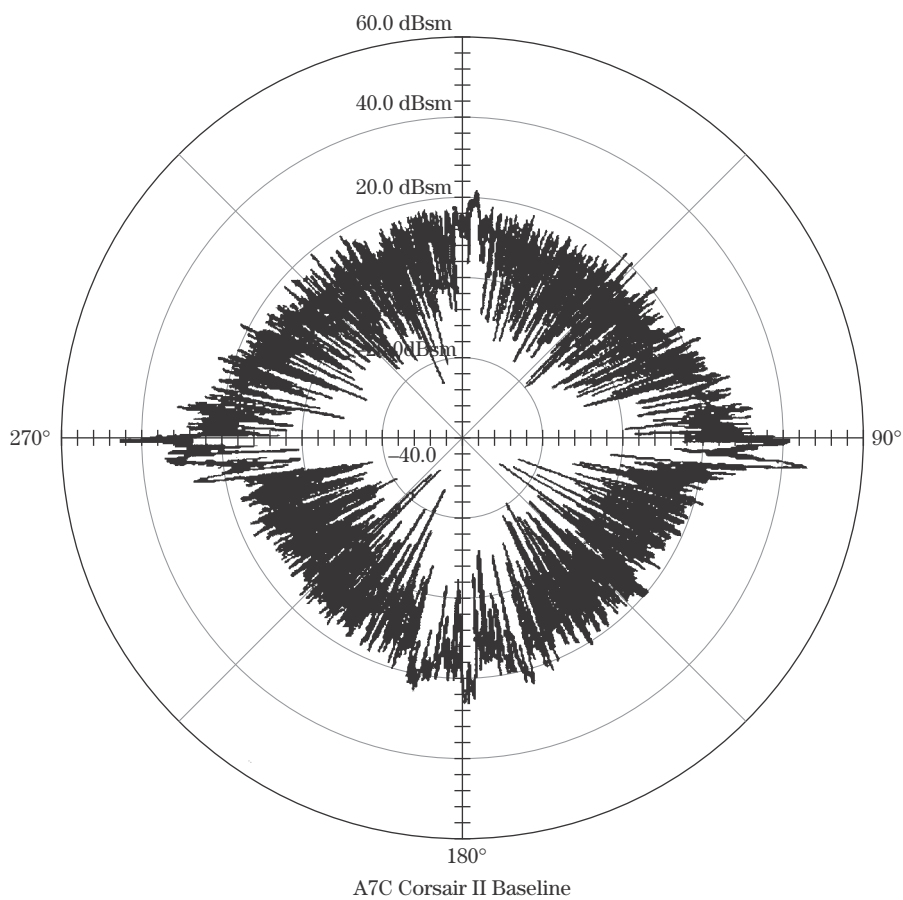
This aircraft at X-band is truly in the optical scattering regime. At each viewing angle it has tens to hundreds of scattering centers that combine in or out of phase to produce the final RCS pattern. Major scattering centers include surfaces normal to the radar line of sight, engine inlet and exhaust cavities, the pilot crew station, control surface edges, avionics antennas and sensors, and the gaps and cracks of construction joints and control surface breaks. Since this vehicle is hundreds of wavelengths long, it does not take much angular movement for these scattering centers to change from adding in phase to adding out of phase with one another. The RCS pattern (Figure 6-30) is very oscillatory and has a rapidly fluctuating backscatter return. While this pattern does not display distinct features, one does see an increase near broadside due to specular scattering. Trailing edge diffraction spikes can also be identified.

Figure 6-31, an image of the scattering centers when the radar is perpendicular to the wing leading edge, shows numerous scattering centers. The major ones include the wing leading edge, the pilot crew station region, the engine inlet cowlings, and the engine inlet cavity. The inlet cavity images are off the plan form view at the cross-range location of

**FIGURE 6-29 ■**  
A7C Corsair RCS  
measurement set up  
at the Navy Junction  
Ranch Range.



**FIGURE 6-30 ■**  
A7 C measured  
backscatter for  
horizontal  
polarization at  
9.5 GHz, 20 dB/div.





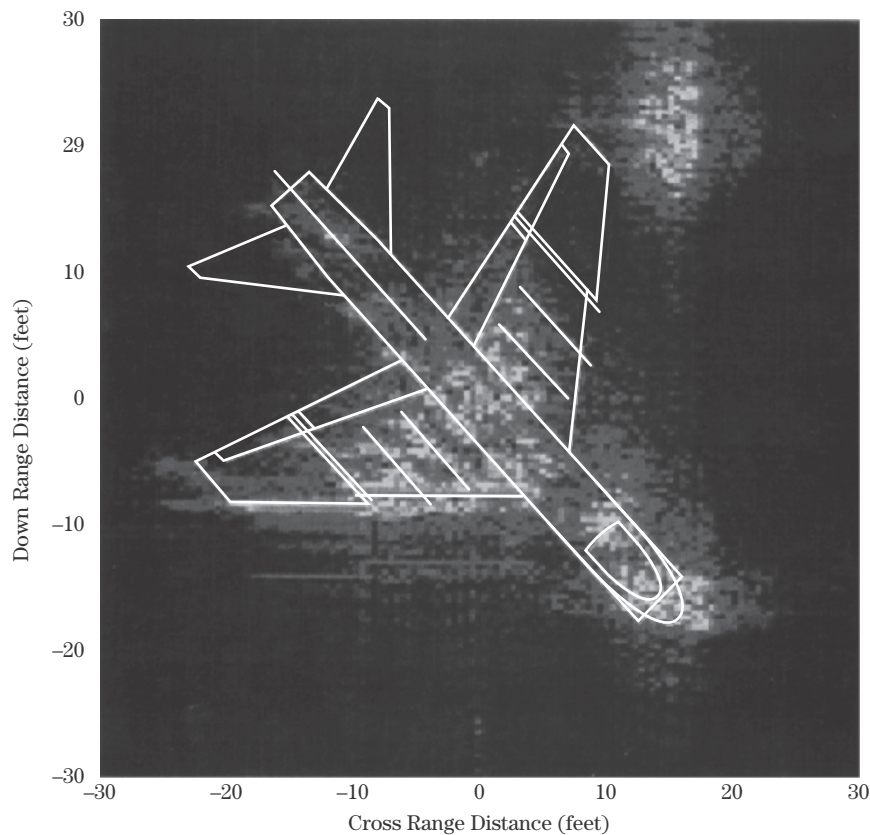


**FIGURE 6-31** ■  
A7 down/cross  
range image  
measurements when  
perpendicular to  
wing leading edge  
for horizontal  
polarization at  
X-band [Navy  
Junction Range  
Range].

the engine inlet and at a down-range location corresponding to the engine front face. Note that this cavity return is one of the major scattering centers at this viewing angle.

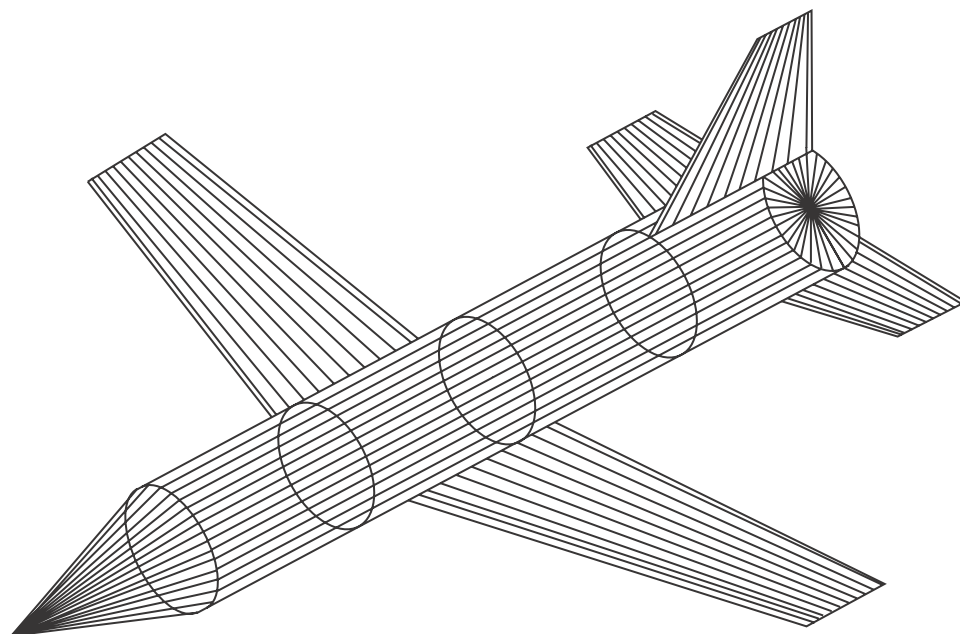
The last example is a “stove pipe” aircraft (Figure 6-32). The model is approximately 3 feet long and was measured at C-band, horizontal polarization, along with image measurements of the scattering centers at various aspect angles. Figure 6-33 shows the measured backscatter RCS (left half of the figure) along with a high-frequency computer physical optics code prediction (right half of the figure). The measurements and the optics prediction code show reasonable agreement, as should be the case since this RCS target measurement is in the optics regime. Specific specular scattering centers as a function of aspect angle—such as the cylinder broadside and vertical tail return, tail flat disk return, nose cone return, and wing leading-edge returns—can be seen on the polar plot.

Image measurements were also performed for a number of aspect angles (Figures 6-34 through 6-38). In these images, the radar is below the picture so that down-range (time delay) is up the page and cross-range is left or right. Target rotation allows for cross-range processing, and radar bandwidth allows for down-range image processing [8].

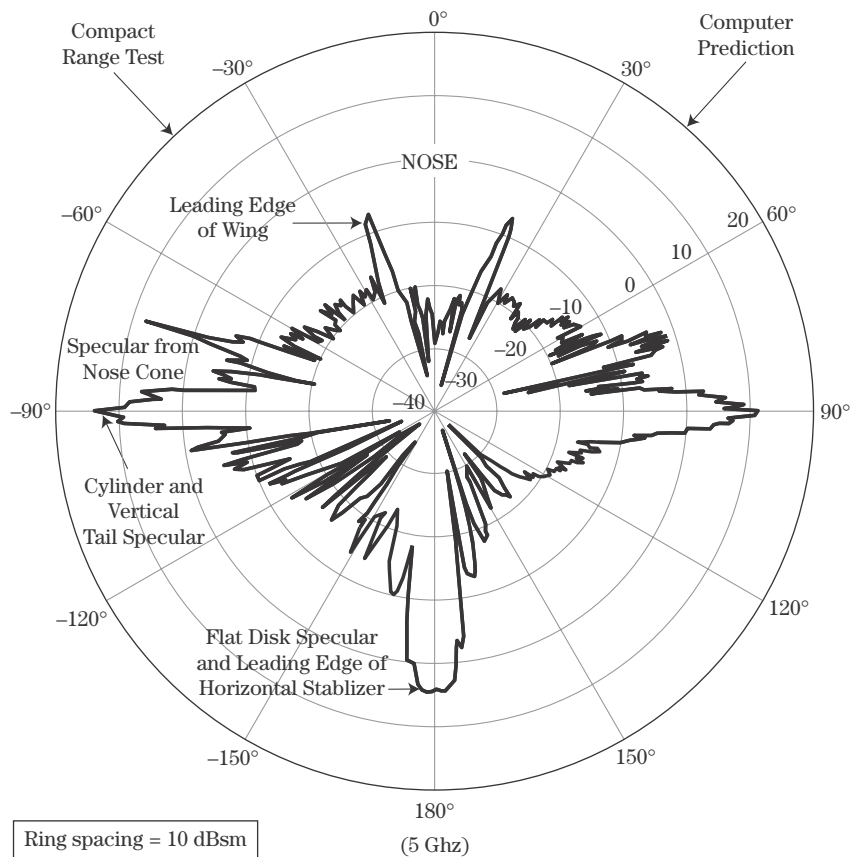
The nose-view scattering center image (Figure 6-34) shows the scattering centers to be the discontinuity between the nose cone and cylinder (the line of sight is perpendicular to the rim edge), the trailing edge of the vertical fin (trailing edge diffraction for horizontal polarization), and cylinder surface traveling wave energy reflecting from the forward wing



**FIGURE 6-32 ■**  
“Stovepipe” RCS  
backscatter model.



**FIGURE 6-33 ■**  
Measured and  
Physical Optics  
predicted RCS for  
“Stovepipe”  
geometry at C band.



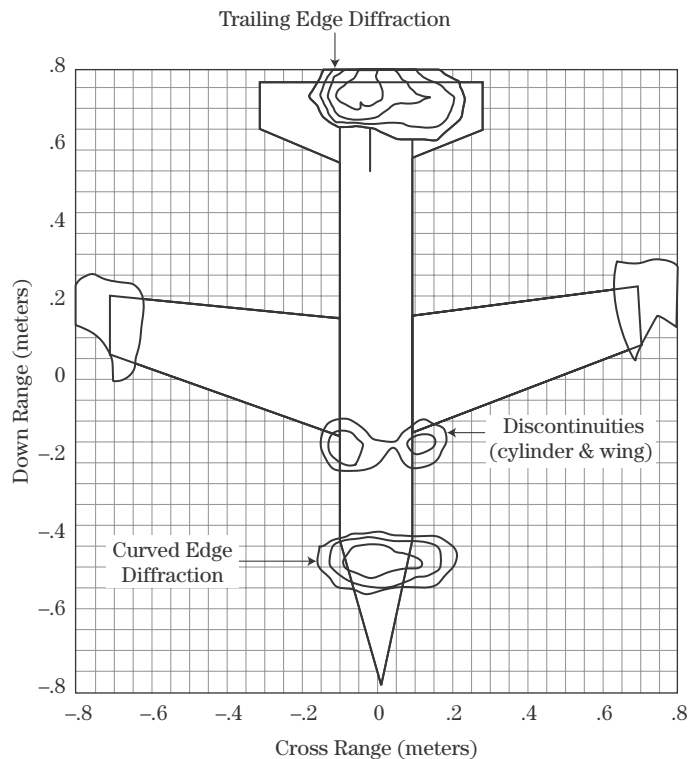


**FIGURE 6-34** ■  
“Stovepipe” nose  
view scattering  
centers.

root. These four major scattering centers combine in or out of phase to give the 0 degree net RCS value of approximately  $-25$  dBsm seen in Figure 6-33.

Broadside-view scattering centers (Figure 6-35) are the cylinder sides, the vertical edge of the vertical fin, and the vertical surface of the tail fin. Note that, for horizontal polarization, the wing partially shadows the cylinder.

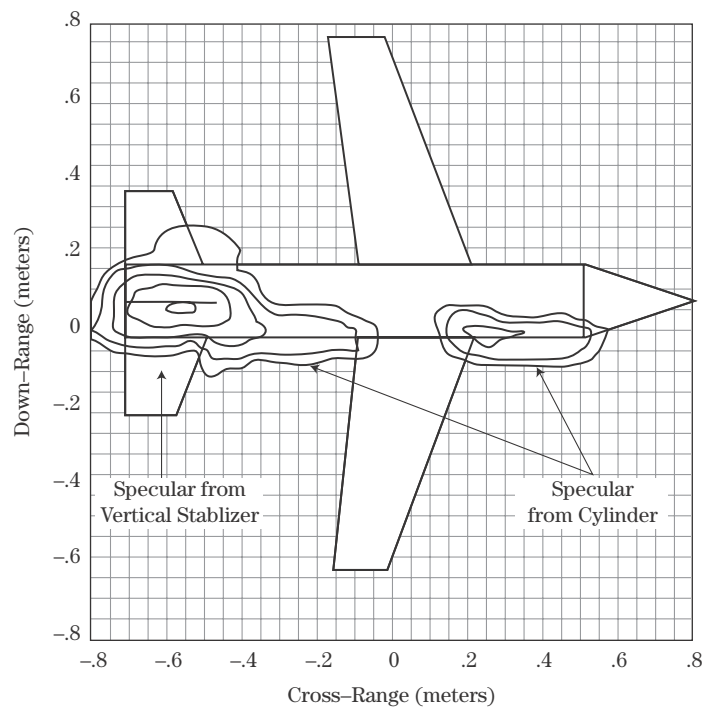
Tail-view scattering centers (Figure 6-36) are the flat disk specular scattering at the end of the cylinder, the edge diffraction from the horizontal stabilizer (horizontal polarization), several very small traveling-wave scattering mechanisms from energy going down the sides of the cylinder and across the vertical fin surfaces, and remnants of wing-edge diffraction.

Scattering centers when the model is viewed perpendicular to the wing leading edge (Figure 6-37) are the wing-edge diffraction (electric field parallel to the edge) and the vertical fin trailing edge (electric field perpendicular to the edge).

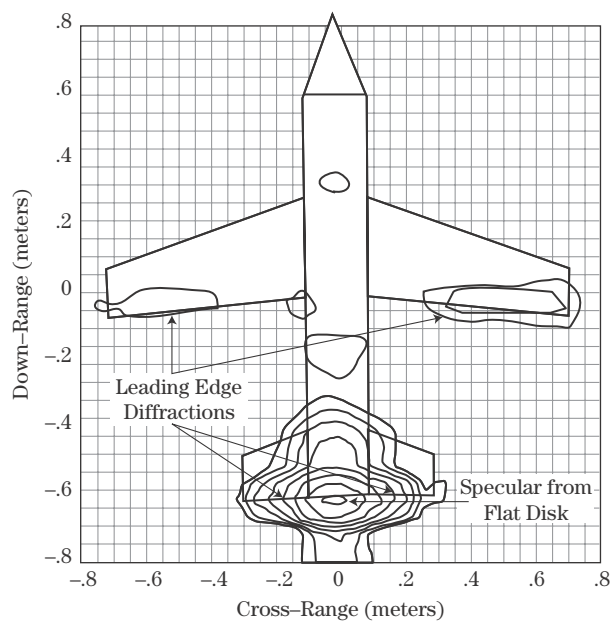
The last view is from an aspect perpendicular to the front nose cone (Figure 6-38). Now the scattering centers are the specular return from the single-curved nose cone surface and the edge diffraction from the trailing edge of the vertical fin (electric field perpendicular to edge).

This stove pipe geometry shows that electromagnetic backscattering is very much a geometry issue; that is, scattering centers appear when surfaces or edges are perpendicular to the radar. These images also show that scattering centers in the optical regime are local and that they are dependent on geometry, radar orientation, and polarization. If the images were formed at X-band rather than C-band, the scattering centers would be very similar since the geometry is the same. Only the magnitude of the frequency dependent scattering mechanisms would be different.

**FIGURE 6-35 ■**  
“Stovepipe”  
broadside view  
scattering centers.



**FIGURE 6-36 ■**  
“Stovepipe” tail view  
scattering centers.



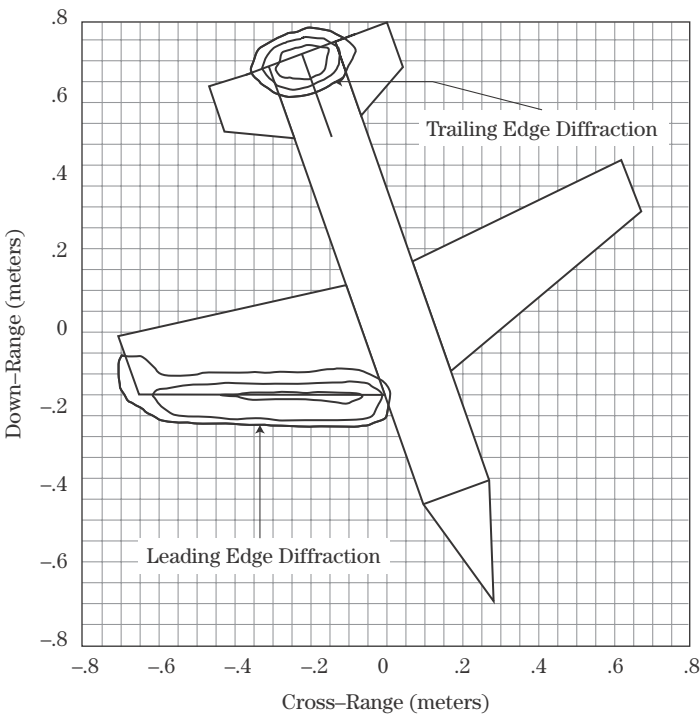


**FIGURE 6-37** ■  
“Stovepipe” wing  
leading edge view  
scattering centers.

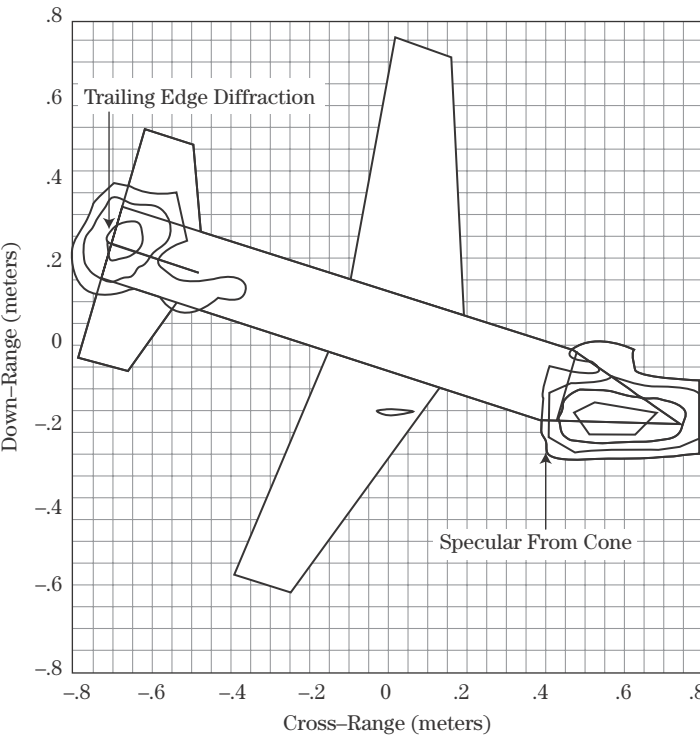


**FIGURE 6-38** ■  
“Stovepipe”  
scattering centers  
when viewed normal  
to front nose cone.

## 6.7 | FURTHER READING

There are several classic and modern textbooks on radar cross section theory, phenomenology, measurement, and prediction. The most modern, and perhaps the best introduction to the subject, is the text by Knott et al. [1]. Other comprehensive sources include Jenn [9] and the two-volume *Radar Cross Section Handbook* [10]. More theoretical treatments are available in Crispin and Siegel [11], Ogilvy [12], Maffett [13], and Ross Stone [14].

RCS reduction is a topic of great interest in military applications. An excellent introduction is available in [1], with additional detail provided in the text by Bhattacharyya and Sengupta [15]. Vinoy and Jha [16] discuss the particular method of using radar-absorbing materials for RCS reduction.

## 6.8 | REFERENCES

- [1] Knott, E.F., Shaeffer, J.F., and Tuley, M.T., *Radar Cross Section*, 2d ed., Scitech Publishing, Raleigh, NC, 2004.
- [2] Emmons, G.A., and Alexander, P.M., "Polarization Scattering Matrices of Polarimetric Radar," Technical Report RE-83-1, U.S. Army Missile Command, Redstone Arsenal, AL, March 1983.
- [3] Knott, E.F., "Radar Cross Section Short Course Notes," Georgia Institute of Technology, Atlanta, 1984.
- [4] Jay, F. (Ed.), *IEEE Standard Dictionary of Electrical and Electronic Terms*, ANSI/IEEE Std 100-1984, 3d ed., IEEE Press, New York, 1984.
- [5] Ruck, G.T. (Ed.), *Radar Cross Section Handbook*, vols. 1 and 2, Plenum Press, New York, 1970.
- [6] Keller, J.B., "Geometrical Theory of Diffraction," *Journal of the Optical Society of America*, vol. 52, p. 116, 1962.
- [7] Ross, R.A., "Radar Cross Section of Rectangular Flat Plates as a Function of Aspect Angle," *IEEE Transactions on Antennas and Propagation*, vol. AP-14, pp. 329–335, May 1966.
- [8] Mensa, D. L., *High Resolution Radar Imaging*, Artech House, Norwood, MA, 1981.
- [9] Jenn, D.C., *Radar and Laser Cross Section Engineering*, American Institute of Aeronautics and Astronautics, Reston, VA, 1995.
- [10] Ruck, G.T., Barrick, D.E., Stuart, W.D., and Krichbaum, C.K., *Radar Cross Section Handbook*, vols. 1 and 2, Plenum Press, New York, 1970.
- [11] Crispin, J.W., and Siegel, K.M., *Methods of Radar Cross Section Analysis*, Academic Press, New York, 1968.
- [12] Ogilvy, J.A., *Theory of Wave Scattering From Random Rough Surfaces*, Taylor & Francis, Philadelphia, 1991.
- [13] Maffett, A.L., *Topics for a Statistical Description of Radar Cross Section*, John Wiley & Sons, New York, 1989.
- [14] Ross Stone, W., *Radar Cross Sections of Complex Objects*, IEEE Press, New York, 1990.
- [15] Bhattacharyya, A.K., and Sengupta, D.L., *Radar Cross Section Analysis and Control*, Artech House, Boston, 1991.
- [16] Vinoy, K.J., and Jha, R.M., *Radar Absorbing Materials*, Kluwer Academic Publishers, Boston, 1996.

## 6.9 | PROBLEMS

1. For specular scattering, what is the key geometric concept involving the transmitter, receiver, and target surface?
2. What is specular backscatter?
3. Where in space do edge normals point?
4. What is the direction of target surface normals for (a) specular backscatter and (b) edge normals?
5. Why can RCS be measured using either  $E$  or  $H$  fields?
6. What scattering mechanisms do not depend on polarization?
7. What scattering mechanisms do depend on polarization?
8. In free space, how much of the EM wave energy is in the  $E$  field? In the  $H$  field?
9. Near a PEC surface, which EM wave field component contains most of the energy and why?
10. For an EM wave propagating inside a material medium, what physical properties of the material determine the velocity of propagation?
11. How does the wavelength of an EM wave inside of a material differ from that of free space?
12. If you are designing an outdoor measurement range for RCS with a specified error tolerance, what level of background RCS would you try to achieve? Why?
13. What was Maxwell's key contribution such that the EM laws of Gauss, Ampere, and Faraday became collectively known as Maxwell's Equations?
14. For an EM wave propagating toward a PEC surface, what happens to the impedance of the wave very close to the PEC surface?
15. In world of computational EM, if an aircraft model has its fuselage along the  $x$  axis and its wings parallel to the  $x$ - $y$  plane, what spherical unit vectors correspond to horizontal and vertical polarization for an angle cut in the  $x$ - $y$  plane?
16. When can a spherically spreading EM wave be characterized as a plane wave?
17. What are the EM fields inside a closed PEC surface?
18. What is the polarization scattering matrix?
19. Can a scattering-only measurement ever tell us more about a target at a fixed angle than the PSM?
20. For circular polarization, what is the reference for deciding whether a wave is left or right circularly polarized?
21. In Rayleigh region scattering, what is the phase variation of the incident wave over the target?
22. In high-frequency scattering, why does the backscatter RCS usually vary so rapidly with target movement?
23. What is the most important feature of specular scattering from (a) planar surfaces, (b) single-curved surfaces, and (c) double-curved surfaces?
24. If you were to design a target to have low specular RCS, how would you proceed?
25. The formula for the magnitude of specular scattering has an area term. In the backscatter case, what area is this?